hep-ph/0408142
TUM-HEP-551/04
PITHA-04/13

August 10, 2004

$K^+ \to \pi^+\nu\bar{\nu}$ and $K_{\rm L} \to \pi^0\nu\bar{\nu}$ Decays in the General MSSM

Andrzej J. Buras[1], Thorsten Ewerth[1], Sebastian Jäger[1,2], and Janusz Rosiek[1,3]

[1] Physik Department, Technische Universität München,
D-85748 Garching, Germany
[2] Institut für Theoretische Physik E, RWTH Aachen
D-52056 Aachen, Germany
[3] Institute of Theoretical Physics, Warsaw University
Hoża 69, 00-681 Warsaw, Poland

Abstract

We reanalyze the rare decays $K^+ \to \pi^+\nu\bar{\nu}$ and $K_{\rm L} \to \pi^0\nu\bar{\nu}$ in a general MSSM with conserved R-parity. Working in the mass eigenstate basis and performing adaptive scanning of a large space of supersymmetric parameters, 16 parameters in the constrained scan and 63 in the extended scan, we find that large departures from the Standard Model expectations are possible while satisfying all existing constraints. Both branching ratios can be as large as a few times 10^{-10} with $Br(K_{\rm L} \to \pi^0\nu\bar{\nu})$ often larger than $Br(K^+ \to \pi^+\nu\bar{\nu})$ and close to its model independent upper bound. We give examples of supersymmetric parameters for which large departures from the SM expectations can be found and emphasize that the present 90% C.L. experimental upper bound on $Br(K^+ \to \pi^+\nu\bar{\nu})$ gives a non trivial constraint on the MSSM parameter space. Unlike previous analyses, we find that chargino box diagrams can give, already for moderately light charged sleptons, a significant contribution. As a byproduct we find that the ranges for the angles β and γ in the unitarity triangle are relaxed due to the presence of new CP-violating phases in $K^0 - \bar{K}^0$ and $B_d^0 - \bar{B}_d^0$ mixing to $12^\circ \le \beta \le 27^\circ$ and $20^\circ \le \gamma \le 110^\circ$.

1 Introduction

The rare decays $K^+ \to \pi^+\nu\bar{\nu}$ and $K_{\rm L} \to \pi^0\nu\bar{\nu}$ belong to the theoretically cleanest processes in the field of meson decays. In fact their branching ratios can be computed to an exceptionally high degree of precision that is not matched by any other decay of mesons [1, 2, 3, 4, 5]. A detailed review of $K \to \pi\nu\bar{\nu}$ decays within the Standard Model (SM) and its extensions has been recently presented in [6], where an extensive list of relevant papers can be found. Earlier reviews have been given in [7, 8].

As emphasized in [6], the clean theoretical character of these decays remains valid in essentially all extensions of the SM, whereas this is generally not the case for non-leptonic two-body B decays used to determine the CKM parameters through CP asymmetries and/or other strategies. While several mixing induced CP asymmetries in non-leptonic B decays within the SM are essentially free from hadronic uncertainties [9], as the latter cancel out due to the dominance of a single CKM amplitude, this is often not the case in extensions of the SM in which the amplitudes receive new contributions with different weak phases implying no cancellation of hadronic uncertainties in the relevant observables [10, 11].

In this context an important virtue of $K \to \pi\nu\bar{\nu}$ decays is the possibility of parametrizing the new physics contributions to their branching ratios, in essentially all extensions of the SM, in a model-independent manner by just two parameters [12], the magnitude of the short distance function X and its complex phase:

$$X = |X|e^{i\theta_X} \tag{1.1}$$

with $|X| = X(x_t)$ and $\theta_X = 0$ in the SM. Here $x_t = m_t^2/M_W^2$.

The most recent predictions for the relevant branching ratios within the SM read [6]

$$Br(K^+ \to \pi^+\nu\bar{\nu})_{\rm SM} = (7.8 \pm 1.2) \cdot 10^{-11}, \tag{1.2}$$

$$Br(K_{\rm L} \to \pi^0\nu\bar{\nu})_{\rm SM} = (3.0 \pm 0.6) \cdot 10^{-11}, \tag{1.3}$$

in the ballpark of other estimates [8, 13, 14, 15, 16]. As discussed in [6] a NNLO calculation of the charm contribution to $K^+ \to \pi^+\nu\bar{\nu}$ and further progress on the determination of the CKM parameters coming in the next few years dominantly from BaBar, Belle, Tevatron and later from LHC and BTeV, should eventually allow predictions for $Br(K^+ \to \pi^+\nu\bar{\nu})$ and $Br(K_{\rm L} \to \pi^0\nu\bar{\nu})$ with uncertainties of at most $\pm 5\%$.

On the experimental side the two events observed by the AGS E787 collaboration at Brookhaven [17, 18] and the additional event observed by AGS E949 [19] imply

$$Br(K^+ \to \pi^+\nu\bar{\nu}) = (14.7^{+13.0}_{-8.9}) \cdot 10^{-11}. \tag{1.4}$$

While the central value in (1.4) is about a factor of two higher than the SM value, the large experimental error precludes any claims for signals of new physics in the $K^+ \to \pi^+\nu\bar{\nu}$ data. Further progress is expected in principle from AGS E949, from the efforts at Fermilab around the CKM experiment [20], the corresponding efforts at CERN around the NA48 collaboration [21] and at JPARC in Japan [22]. Hopefully this will bring additional 50-100 events in the next five years.

On the other hand the present experimental upper bound on $Br(K_{\rm L} \to \pi^0\nu\bar{\nu})$ from KTeV [23] reads

$$Br(K_{\rm L} \to \pi^0\nu\bar{\nu}) < 5.9 \times 10^{-7}. \tag{1.5}$$

This is about four orders of magnitude above the SM expectation but a $K_{\rm L} \to \pi^0\nu\bar{\nu}$ experiment at KEK, E391a [24], which recently took data, should in its first stage improve the bound in (1.5) by three orders of magnitude. While this is insufficient to reach the SM level, a few events could be observed if $Br(K_{\rm L} \to \pi^0\nu\bar{\nu})$ turned out to be by one order of magnitude larger due to new physics contributions. Further progress on this decay is expected from KOPIO [25] at Brookhaven, and from the second stage of the E391 experiment at JPARC [22], that could in principle provide a few hundreds of $K_{\rm L} \to \pi^0\nu\bar{\nu}$ SM events, which would be truly fantastic!

In this context let us recall that a model-independent upper bound on $Br(K_{\rm L} \to \pi^0\nu\bar{\nu})$ following from isopin symmetry reads [26]

$$Br(K_{\rm L} \to \pi^0\nu\bar{\nu}) < 4.4 \cdot Br(K^+ \to \pi^+\nu\bar{\nu}). \tag{1.6}$$

With the data in (1.4), which imply [19]

$$Br(K^+ \to \pi^+\nu\bar{\nu}) < 3.8 \cdot 10^{-10} \ (90\% \ \text{C.L.}), \tag{1.7}$$

one finds then (1.6)

$$Br(K_{\rm L} \to \pi^0\nu\bar{\nu}) < 1.7 \cdot 10^{-9} \ (90\% \ \text{C.L.}), \tag{1.8}$$

still two orders of magnitude below the upper bound from the KTeV experiment in (1.5).

Recently it has been pointed out in [15, 16] that the anomalies seen in the $B \to \pi K$ data may imply a significantly enhanced value of $|X|$ and a large complex phase θ_X:

$$|X| = 2.17 \pm 0.12, \qquad \theta_X = -(86 \pm 12)^\circ, \tag{1.9}$$

to be compared with $X = 1.53 \pm 0.04$ and $\theta_X = 0$ in the SM.

The implications of this possibility are spectacular:

$$Br(K^+ \to \pi^+\nu\bar{\nu}) = (7.5 \pm 2.1) \cdot 10^{-11}, \tag{1.10}$$

$$Br(K_{\rm L} \to \pi^0\nu\bar{\nu}) = (3.1 \pm 1.0) \cdot 10^{-10}. \tag{1.11}$$

Consequently, while $Br(K_{\rm L} \to \pi^0\nu\bar{\nu}) \approx (1/3)Br(K^+ \to \pi^+\nu\bar{\nu})$ in the SM, it is substantially larger than $Br(K^+ \to \pi^+\nu\bar{\nu})$ in this scenario. The huge enhancement of $Br(K_{\rm L} \to \pi^0\nu\bar{\nu})$ found in [15, 16] is mainly due to the large weak phase θ_X and its negative sign. One also finds

$$\frac{Br(K_{\rm L} \to \pi^0\nu\bar{\nu})}{Br(K^+ \to \pi^+\nu\bar{\nu})} \approx 4.2 \pm 0.2 \ , \tag{1.12}$$

which means that $Br(K_{\rm L} \to \pi^0\nu\bar{\nu})$ is rather close to its model-independent upper bound in (1.6).

A spectacular implication of these findings is a strong violation of the golden minimal flavour violation relation [27]

$$(\sin 2\beta)_{\pi\nu\bar{\nu}} = (\sin 2\beta)_{\psi K_S}, \tag{1.13}$$

where $-\beta$ is the phase of the V_{td} coupling that could in general be violated by new physics contributions to $K \to \pi\nu\bar{\nu}$ and the asymmetry in $B_d \to \psi K_S$.

Indeed, one finds [15, 16]

$$(\sin 2\beta)_{\pi\nu\bar{\nu}} = \sin 2(\beta - \theta_X) = -(0.69^{+0.23}_{-0.41}), \tag{1.14}$$

in striking disagreement with $(\sin 2\beta)_{\psi K_S} = 0.736 \pm 0.049$. Other interesting implications are discussed in [15, 16, 28, 29].

The analysis in [15, 16] was model independent within a scenario in which new physics manifested itself only through enhanced EW penguins with a new complex phase. This scenario was first considered in [12, 30, 31, 32] in the context of rare K decays and the ratio ε'/ε measuring direct CP violation in the neutral kaon system, and was generalized to rare B decays in [33]. In [15, 16] it has been further generalized to $B \to \pi K$ decays.

The question that we would like to address in the present paper is whether the spectacular effects in $K \to \pi\nu\bar{\nu}$ system found in [15, 16] are still possible within the general MSSM with new sources of flavour violation when all known experimental and theoretical constraints on the relevant parameters are taken into account.

New flavour violating interactions are present in the general MSSM because the sfermion mass matrices can be non-diagonal in the basis in which all quark-squark-neutral-gaugino vertices and quark and lepton mass matrices are flavour diagonal. Instead of diagonalizing sfermion mass matrices it is often convenient to consider their off-diagonal terms as new flavour violating interactions. This so-called mass insertion approximation (MIA) [34] has been reviewed in the classic papers [35, 36, 37], where further references can be found.

In the context of the $K \to \pi\nu\bar{\nu}$ decays the most extensive analyses using the mass insertion method can be found in [38, 12, 30, 32]. It turns out, that sizeable enhancements of $K \to \pi\nu\bar{\nu}$ rates can only be generated by chargino-mediated diagrams with a large LR mixing in the up-squark sector. Reference [32], the most detailed of these papers, finds the upper bounds

$$Br(K^+ \to \pi^+\nu\bar{\nu}) \le 1.7 \cdot 10^{-10}, \qquad Br(K_{\rm L} \to \pi^0\nu\bar{\nu}) \le 1.2 \cdot 10^{-10}. \tag{1.15}$$

Larger values were found rather unlikely. Moreover, as discussed in detail in [12], in these models the minimal flavour violation relation in (1.13) can be violated due to the presence of a new phase θ_X. A rough estimate shows that this phase could be as large as $\pm 25^\circ$. This is not as large as found in [15, 16] but sizable departures from the SM as seen in (1.15) can be found.

However, in [12, 32] the following assumptions (approximations) have been made:

- MIA (up to the second order of expansion) was used in calculation of $K \to \pi\nu\bar{\nu}$ decay rates and other related processes.
- limited number of MSSM parameters, assumed to be most important, were used in numerical scans.
- bounds on mass insertions coming from various experimental results were obtained by the approximate procedure of requiring that each individual term in the mass

insertion expansion at most saturates the measured value; this neglects the possibility of significant cancellations between contributions from different terms in the expansion and also interference with the SM contribution that is always present.

- some additional assumptions not coming from low-energy physics, like GUT induced RGE relations between mass insertions, were taken into account.

The questions that we would like to address here are then, whether by relaxing the assumptions made in [12, 32], going beyond the MIA and performing more extensive numerical scans, while satisfying all existing experimental constraints on supersymmetric parameters,

- θ_X can be as large as found in [15, 16],
- $Br(K^+ \to \pi^+ \nu\bar{\nu})$ can be significantly enhanced over the SM expectations so that it is at least as high as its central experimental value in (1.4),
- $Br(K_{\rm L} \to \pi^0 \nu\bar{\nu})$ can be enhanced by an order of magnitude with the ratio $Br(K_{\rm L} \to \pi^0 \nu\bar{\nu})/Br(K^+ \to \pi^+ \nu\bar{\nu})$ reaching the bound in (1.6).

Moreover, there are the questions:

- In what regions of the parameter space of the general MSSM do the maximal departures from the SM expectations occur?
- What are the bounds on the MSSM parameters implied already by the experimental value on $Br(K^+ \to \pi^+ \nu\bar{\nu})$ in (1.4)?

Answering these questions is a non-trivial numerical task, due to the large number of free parameters and experimental constraints which have to be considered. Here we would like to demonstrate an efficient method of a random scan over the MSSM parameter space, based on an adaptation of the Monte Carlo integration algorithm VEGAS [39, 40]. Such a method is designed to automatically concentrate most of the randomly generated points in the SUSY parameter ranges giving the largest deviations from the SM results, thus allowing for analyzing very large parameter spaces, with 20 or more dimensions, in a reasonable time and without very extensive computer CPU usage. This allows us to answer the first three of the questions listed above. The remaining two points will be discussed elsewhere.

Our paper is organized as follows. In Section 2 we will present the formulae for the branching ratios $Br(K^+ \to \pi^+ \nu\bar{\nu})$ and $Br(K_{\rm L} \to \pi^0 \nu\bar{\nu})$ in terms of the function X, discuss their properties and compare the general MSSM considered here with the simple new physics scenario analyzed in [15, 16]. In Section 3 we discuss the problematic of the huge space of parameters in supersymmetric theories and the method that we propose to tackle this problem. In Section 4 we present our numerical results. Finally, in Section 5 we summarize the main findings of our paper. A list of the contributions to the function X from the relevant box and penguin diagrams is given in an Appendix.

2 Basic Formulae

2.1 Effective Hamiltonian

The effective Hamiltonian relevant for $K^+ \to \pi^+\nu\bar{\nu}$ and $K_{\rm L} \to \pi^0\nu\bar{\nu}$ decays in a general MSSM considered in our paper can be written as follows

$$\mathcal{H}_{\rm eff} = \frac{G_{\rm F}}{\sqrt{2}}\frac{\alpha}{2\pi\sin^2\theta_{\rm w}}\left[\mathcal{H}_{\rm eff}^{(c)} + \mathcal{H}_{\rm eff}^{(t)}\right] \tag{2.1}$$

where the internal charm part

$$\mathcal{H}_{\rm eff}^{(c)} = \sum_{l=e,\mu,\tau} V_{cs}^* V_{cd} X_{\rm NL}^l (\bar{s}d)_{V-A}(\bar{\nu}_l\nu_l)_{V-A} \tag{2.2}$$

is fully dominated by the SM contributions and

$$\mathcal{H}_{\rm eff}^{(t)} = \sum_{l=e,\mu,\tau} V_{ts}^* V_{td}\left[X_L(\bar{s}d)_{V-A}(\bar{\nu}_l\nu_l)_{V-A} + X_R(\bar{s}d)_{V+A}(\bar{\nu}_l\nu_l)_{V-A}\right] \tag{2.3}$$

with X_L receiving both the SM and supersymmetric contributions and X_R only the latter ones that also include charged Higgs exchanges. In the SM X_L is real and given for $\overline{m}_t(m_t) = (168.1 \pm 4.1)$ GeV by

$$X_L^{SM} \equiv X_{SM} = 1.53 \pm 0.04\ . \tag{2.4}$$

The index $l = e,\ \mu,\ \tau$ denotes the lepton flavour. The dependence on the charged lepton mass resulting from the box diagrams is negligible for the top contribution. In the charm sector this is the case only for the electron and the muon but not for the τ-lepton. Below we will give the branching ratios that follow from (2.3).

This parametrization of $\mathcal{H}_{\rm eff}^{(t)}$ is very useful for phenomenological applications and for the comparison with [15, 16], but one should remember that in a general MSSM scenario considered here not all contributions to $\mathcal{H}_{\rm eff}^{(t)}$ are proportional to $V_{ts}^*V_{td}$. This means that parametrizing $\mathcal{H}_{\rm eff}^{(t)}$ as in (2.3), necessarily puts some CKM dependence into X_L and X_R. Therefore we will use below also a different parametrization of new physics contributions.

Now, as the strong interactions are not sensitive to the sign of γ_5, the hadronic matrix elements of $(\bar{s}d)_{V-A}$ and $(\bar{s}d)_{V+A}$ are equal to each other, and consequently the function X playing the central role in our paper is simply given by

$$X = X_L + X_R = |X|e^{i\theta_X}\ . \tag{2.5}$$

Explicit expressions for X_L and X_R are collected in the Appendix. As one can see there, chargino and part of the neutralino contributions to X_R are strongly suppressed by small Yukawa couplings of the down quarks. As we will see, the remaining neutralino contribution proportional to $U(1)$ gauge coupling is typically also much smaller than the dominant terms in X_L, so that $|X_R| \ll |X_L|$ also in the MSSM (except may be for some non-interesting points where X_L is small due to cancellations) and can be neglected for all practical purposes.

2.2 Branching Ratios

The branching ratios for the $K \to \pi\nu\bar{\nu}$ decays, in the new physics scenario considered, can be written as follows [6]

$$Br(K^+ \to \pi^+\nu\bar{\nu}) = \kappa_+ \left[\left(\frac{\mathrm{Im}(\lambda_t X)}{\lambda^5}\right)^2 + \left(\frac{\mathrm{Re}\lambda_c}{\lambda}P_c(X) + \frac{\mathrm{Re}(\lambda_t X)}{\lambda^5}\right)^2\right], \tag{2.6}$$

$$Br(K_{\rm L} \to \pi^0\nu\bar{\nu}) = \kappa_L \left(\frac{\mathrm{Im}(\lambda_t X)}{\lambda^5}\right)^2 \tag{2.7}$$

with $\lambda = 0.224$ being one of the Wolfenstein parameters [41], $\lambda_t = V_{ts}^\star V_{td}$, $\lambda_c = V_{cs}^\star V_{cd}$, κ-factors equal to [6]

$$\kappa_+ = (4.84 \pm 0.06)\cdot 10^{-11}, \qquad \kappa_L = (2.12 \pm 0.03)\cdot 10^{-10} \tag{2.8}$$

and

$$P_c(X) = \frac{1}{\lambda^4}\left[\frac{2}{3}X_{\rm NL}^e + \frac{1}{3}X_{\rm NL}^\tau\right] = 0.39 \pm 0.07 \tag{2.9}$$

resulting from the NLO calculations in [4, 5]. The anatomy of the error in $P_c(X)$ has been recently presented in [6].

As discussed in the next section we will use as our input parameters

$$|V_{us}| = \lambda = 0.224, \qquad |V_{cb}| = A\lambda^2 = 0.0415, \qquad R_b = 0.37 \tag{2.10}$$

where

$$R_b = \frac{(1-\lambda^2/2)}{\lambda}\left|\frac{V_{ub}}{V_{cb}}\right|. \tag{2.11}$$

We recall that A is a Wolfenstein parameter [41] with $A = 0.83 \pm 0.02$ and R_b is one of the sides of the unitarity triangle.

While the parameters in (2.10) contain uncertainties, the latter are sufficiently small so that they can be neglected in comparison with hudge uncertainties in the values of supersymmetric parameters. The choice of these three parameters is dictated by the fact that they are extracted from tree-level decays and consequently their values are not subject to new physics uncertainties.

As the fourth variable we will take the angle γ in the unitarity triangle that is equal to the CKM phase δ_{CKM} in the standard parametrization of this matrix. The angle γ can be in principle measured without any new physics pollution in tree-level B decay strategies that will be only available at LHC and BTeV [9]. In the general MSSM the value of γ may deviate from the one extracted from the usual analysis of the unitarity triangle that uses SM expressions. For this reason we will allow γ to vary in the full range

$$-180^\circ \le \gamma \le 180^\circ, \tag{2.12}$$

but as we will see in Section 4, only the range $20^\circ \le \gamma \le 110^\circ$ is allowed when all constraints are taken into account.

We define next $\overline{X}_{SUSY}$ through

$$\lambda_t X = \lambda_t X_{SM} + \lambda^5 \overline{X}_{SUSY} \tag{2.13}$$

and introduce

$$a = P_c(X) + \frac{|V_{cb}|^2}{\lambda^4} X_{SM} \approx 1.43, \qquad b = R_b \frac{|V_{cb}|^2}{\lambda^4} X_{SM} \approx 0.39, \tag{2.14}$$

that do not depend on supersymmetric parameters. We find then

$$Br(K^+ \to \pi^+ \nu\bar{\nu}) = \kappa_+ \left[(Q_{eff}(\gamma) + \mathrm{Im}\overline{X}_{SUSY})^2 + (P_{eff}(\gamma) - \mathrm{Re}\overline{X}_{SUSY})^2 \right], \tag{2.15}$$

$$Br(K_{\mathrm{L}} \to \pi^0 \nu\bar{\nu}) = \kappa_L \left(Q_{eff}(\gamma) + \mathrm{Im}\overline{X}_{SUSY} \right)^2 , \tag{2.16}$$

where

$$P_{eff}(\gamma) = (1 - \frac{\lambda^2}{2}) \left[a - b\cos\gamma \right], \qquad Q_{eff}(\gamma) = b \sin\gamma \, . \tag{2.17}$$

As $P_{eff}(\gamma)$ and $Q_{eff}(\gamma)$ can be fully determined within the SM, provided γ can be measured through tree-level decays, the formulae (2.15) and (2.16) transparently exhibit supersymmetric contributions. With $\gamma \approx 65^\circ$ we have

$$P_{eff}(\gamma) \approx 1.23, \qquad Q_{eff}(\gamma) \approx 0.35 \, . \tag{2.18}$$

2.3 Comparison with [16]

In order to compare our results with the ones in [16], it is useful to have the expressions for both branching ratios in terms of R_t and β, where β is another angle and R_t another side of the unitarity triangle.

Now, for each pair (R_b, γ), used above, one can determine the pair (R_t, β) through

$$R_t = \sqrt{1 + R_b^2 - 2R_b \cos\gamma}, \qquad \cot\beta = \frac{1 - R_b\cos\gamma}{R_b \sin\gamma} \tag{2.19}$$

and consequently calculate both branching ratios by using

$$Br(K^+ \to \pi^+ \nu\bar{\nu}) = \kappa_+ \left[\tilde{r}^2 A^4 R_t^2 |X|^2 + 2\tilde{r}\bar{P}_c(X) A^2 R_t |X| \cos\beta_X + \bar{P}_c(X)^2 \right] \tag{2.20}$$

$$Br(K_{\mathrm{L}} \to \pi^0 \nu\bar{\nu}) = \kappa_L \tilde{r}^2 A^4 R_t^2 |X|^2 \sin^2\beta_X, \tag{2.21}$$

where

$$\bar{P}_c(X) = \left(1 - \frac{\lambda^2}{2} \right) P_c(X), \tag{2.22}$$

$$\beta_X = \beta - \beta_s - \theta_X, \qquad \tilde{r} = \left| \frac{V_{ts}}{V_{cb}} \right| \approx 0.985, \tag{2.23}$$

$$V_{td} = A R_t \lambda^3 e^{-i\beta}, \qquad V_{ts} = -|V_{ts}| e^{-i\beta_s}. \tag{2.24}$$

The small phase $\beta_s \approx -1^\circ$ can be neglected for all practical purposes.

While the formulae (2.20) and (2.21) look exactly as the ones given in [16], there is one important difference that should be empasized here. In the new physics scenario considered in [16] the values of β, R_t and γ were unaffected by new physics contributions and the sole effects of new physics were felt only through $|X|$ and θ_X. In a general MSSM the $a_{\psi K_S}$ asymmetry does not generally measure β but rather $\beta + \theta_d$ with θ_d coming from

new complex contributions in $B_d^0 - \bar{B}_d^0$ mixing. Thus the constraint on the angle β coming from the $a_{\psi K_S}$ asymmetry reads

$$\sin 2(\beta + \theta_d) = 0.736 \pm 0.049 \tag{2.25}$$

so that β could be quite different from $\beta = 23.5^\circ$ found in the SM and used in [16]. Moreover R_t can be modified. Therefore, the comparison of the results obtained here with the ones in [16] requires some care.

3 Numerical analysis

3.1 Independent MSSM parameters

In the general MSSM, the predictions for the branching ratios considered here and various experimental constraints can depend on almost every MSSM parameter. The dependence on the majority of them is weak enough, however, to be safely neglected in principle for the purpose of computing $Br(K_L \to \pi^0 \nu\bar{\nu})$ and $Br(K^+ \to \pi^+ \nu\bar{\nu})$.

Still, parameters may indirectly enter through the expressions for other observables, which we use to constrain the parameter space. Taking a conservative approach we allow for the independent variation of more free parameters than included in the existing literature.

Kobayashi-Maskawa phase	$-180^\circ \leq \gamma \leq 180^\circ$
CP-odd Higgs boson mass	$150 \leq M_A \leq 400$
$SU(2)$ gaugino mass; we use M_1 GUT-related to M_2	$50 \leq M_2 \leq 800$
Gluino mass	$195 \leq m_{\tilde{g}} \leq 2000$
Supersymmetric Higgs mixing parameter	$-400 \leq \mu \leq 400$
Common flavour diagonal slepton mass parameter	$95 \leq M_{sl} \leq 1000$
Common mass parameter for the first two generations of squarks, as well as $\tilde{b}_R$	$240 \leq M_{sq} \leq 1000$
Squark mass parameter for the left stop and sbottom	$50 \leq M_{\tilde{t}_L} \leq 1000$
Squark mass parameter for the right stop	$50 \leq M_{\tilde{t}_R} \leq 1000$
Flavour universal trilinear scalar mixing parameter (normalized to the fermion mass)	$-1 \leq A \leq 1$
Mass insertion δ^{12}_{LL}	$\lvert\delta^{12}_{LL}\rvert \leq 0.135$
Mass insertion δ^{13}_{ULR}	$\lvert\delta^{13}_{ULR}\rvert \leq 1.65$
Mass insertion δ^{23}_{ULR}	$\lvert\delta^{23}_{ULR}\rvert \leq 1.65$

Table 1: Parameters and their ranges used in the "constrained" scan (16 real degrees of freedom). All mass parameters are in GeV.

To start with, we assume that $Br(K_L \to \pi^0\nu\bar{\nu})$ and $Br(K^+ \to \pi^+\nu\bar{\nu})$ may depend significantly on the set of unknown SM and SUSY parameters listed in Table 1. We took as fixed the other SM parameters, including fermion masses and the CKM parameters given in (2.10), as their measurements are known to be relatively insensitive to physics beyond the SM. This leaves as our only free SM parameter the CKM angle γ, which to date has not been determined from tree-level decays.

Apart from the flavour diagonal supersymmetric mass parameters, we vary several off-diagonal ones. For a transparent parameterization and easy comparison with the literature, it is useful to define mass insertions, even though our actual computation makes use of exactly diagonalized sfermion, chargino, and neutralino mass matrices. Following [35, 36], we define

$$\delta^{IJ}_{SXY} = \frac{(M^2_S)^{IJ}_{XY}}{\sqrt{(M^2_S)^{II}_{XX}\,(M^2_S)^{JJ}_{YY}}}. \tag{3.1}$$

Here I, J denote quark flavours, X, Y the (superfield) chirality, and the "sector" S can be either U or D. Evidently, this definition depends on the basis chosen in flavour space. For the right-handed up and down squarks, there exists a preferred choice selected by the mass eigenstates of their respective SM partners. In the left-handed sector this is different, because $SU(2)$ invariance dictates that the MSSM Lagrangian contains only one soft mass matrix for the doublet squarks. This implies that δ^{IJ}_{ULL} and δ^{IJ}_{DLL} are related. In the super-CKM basis, where each squark field is the superpartner of a quark mass eigenstate, this correspondence is given by CKM matrix elements. As a consequence, even for diagonal $(M^2_D)^{IJ}_{LL}$ the off-diagonal δ^{IJ}_{ULL} are in general nonzero in this basis. Also, the mixings and mass splittings among left-handed up squarks are constrained by bounds on down-squark mixings from $K^0 - \bar{K}^0$ mixing.

In the context of $K \to \pi\nu\bar{\nu}$, it has been pointed out by the authors of [12] that a particularly useful choice of basis is one where the left-handed up squark basis states are simply the $SU(2)$ partners of the left-handed down squarks, which in turn are the superpartners of the left-handed down-type quarks, so that the gluino and neutralino couplings are flavour conserving. This eliminates the CKM elements from the chargino couplings to the left-handed up squarks, and in particular from the term in the MIA that is believed to be dominant [30]. Besides, such a basis ensures that any choice of δ's automatically preserves $SU(2)$ invariance. We use this basis, to be called the BRS basis, in presenting our results in this paper. We also omit the "sector" index on the δ_{LL}.

The decays $K_L \to \pi^0\nu\bar{\nu}$ and $K^+ \to \pi^+\nu\bar{\nu}$ are $\Delta S = 1$ processes and correspond to a transition between the first and second quark generations. Thus, they could certainly depend on (12) squark mass insertions. However, as pointed out in [30], both decays are sensitive also to second-order terms in the mass insertion expansion, namely, to products of a (13) and (the conjugate of) a (23) mass insertion. Therefore, we start from varying independently five (12) mass insertions, δ^{12}_{LL}, δ^{12}_{DRR}, δ^{12}_{URR}, δ^{12}_{DLR} and δ^{12}_{ULR}, plus five more (13) and five (23) mass insertions (assuming for the moment that all LR mass insertions are hermitian, e.g. $\delta^{13}_{DLR} = \delta^{31\star}_{DLR}$).

Even assuming that all flavour diagonal quantities from the list above are real (there is no reason to constrain mass insertions to be real), we have listed already 40 free real parameters. This is a huge number for any reasonably dense numerical scan. To avoid excessive computation time, we first tested how sensitive to the various mass insertions

the predictions for our branching ratios really are. In Fig. 1 we plot the dependence of $Br(K^+ \to \pi^+\nu\bar{\nu})$ on δ^{12}_{LL} and the product $\delta^{13}_{ULR}\delta^{23\star}_{ULR}$ for a chosen set of SUSY parameters. The dependence on the other mass insertions, not shown in the plots, is much weaker and can be neglected in the first approximation.

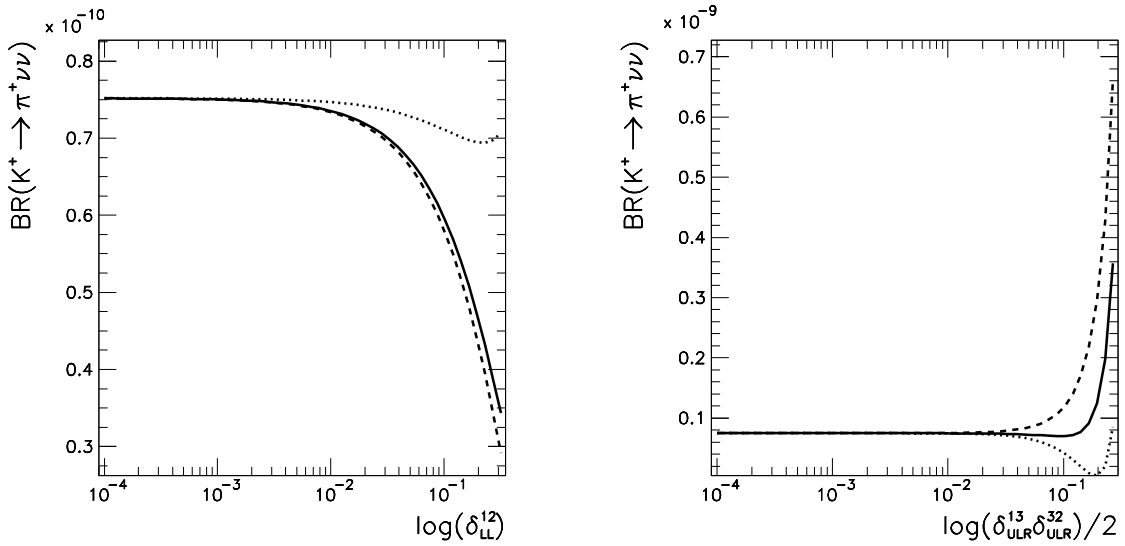

Figure 1: Dependence of $Br(K^+ \to \pi^+\nu\bar{\nu})$ on chosen mass insertions for $\gamma = 65°$, $\tan\beta = 2$, $M_{sq} = M_{\tilde{t}_L} = M_{\tilde{t}_R} = 500$, $M_{sl} = 300$, $M_2 = 200$, $m_{\tilde{g}} = 3M_2$, $\mu = 100$, $M_A = 200$ (all masses in GeV). Solid, dashed and dotted lines: δ^{12}_{LL} and $\delta^{13}_{ULR}\delta^{32}_{ULR}$ complex, real and imaginary, respectively.

Fig. 1 suggests that it is sufficient in the numerical scan to vary only three independent mass insertions, δ^{12}_{LL}, δ^{13}_{ULR} and δ^{23}_{ULR}. In fact the dependence on δ^{12}_{LL}, which is tightly constrained from mixing in the neutral kaon system, is almost negligible for realistic values.

Also, as we tested, both branching ratios in question are only weakly sensitive to GUT- or SUGRA-type assumptions concerning relations between SUSY mass parameters (e.g unified gaugino masses or sfermion mass parameters). Thus, the large but already numerically more feasible total number of 16 free parameters appears to be sufficient to explore the possible ranges of $Br(K^+ \to \pi^+\nu\bar{\nu})$ and $Br(K_L \to \pi^0\nu\bar{\nu})$ in the framework of the MSSM. However, this is not true when trying to satisfy experimental bounds and selecting allowed values of the SUSY parameters. For example, keeping the product $\delta^{13}_{LL}\delta^{23\star}_{LL}$ constant but varying δ^{13}_{LL} independently does not affect $Br(K^+ \to \pi^+\nu\bar{\nu})$ and $Br(K_L \to \pi^0\nu\bar{\nu})$ but allows to satisfy bounds coming from ΔM_d, the measured $B^0_d - \bar{B}^0_d$ mass difference. This motivates keeping, in δ^{12}_{LL}, one more flavour violating parameter even in the "minimal" 16-parameter scan. Later, we will see that our numerical method is powerful enough to study the consequences of further increasing the number of degrees of freedom, which turn out to be unimportant.

3.2 Theoretical and experimental bounds

The enormous freedom in the SUSY parameter space is reduced by a number of phenomenological constraints the theory must satisfy. From the experimental side we take into account the set of bounds and measurements listed in Table 2. As can be seen, we do not take into account the ε'/ε constraint, as its calculation still has very large theoretical uncertainities. Doing this we are aware of the fact that ε'/ε could one day offer a very powerful constraint on the size of SUSY contributions [31, 32].

Quantity	Measured value	Experimental error
Lightest neutralino mass	> 46.0 GeV	
Second lightest neutralino mass	> 62.4 GeV	
Lightest chargino mass	> 94.0 GeV	
The two "sbottom" masses	> 89.0 GeV	
The two "stop" masses	> 95.7 GeV	
all other squark masses	> 250.0 GeV	
$\lvert\varepsilon_K\rvert$	$2.280 \cdot 10^{-3}$	$0.013 \cdot 10^{-3}$
ΔM_K	$3.489 \cdot 10^{-15}$ GeV	$0.008 \cdot 10^{-15}$
ΔM_d	$3.31 \cdot 10^{-13}$ GeV	$0.04 \cdot 10^{-13}$
ΔM_s	$> 9.5 \cdot 10^{-12}$ GeV	
$Br(B_s \to X_s\gamma)$	$3.28 \cdot 10^{-4}$	$^{+0.41}_{-0.36} \cdot 10^{-4}$
$(\sin 2\beta)_{\psi K_S}$	0.736	0.049

Table 2: Experimental measurements used to constrain the MSSM parameter space. Limits on supersymmetric particles masses published in [42] are used. The quotes on "sbottom" and "stop" indicate that these are only approximate flavour states.

Due to the large number of unknown parameters and substantial theoretical uncertainities present in many calculations, it is pointless (and certainly very difficult to implement from a practical point of view) to use everywhere the state-of-art calculations of higher order QCD corrections and other non-leading effects calculated in the literature. Nevertheless, whenever feasible we try to avoid unnecessary simplifications made in many papers. In particular:

- For low energy FCNC and CP violating processes, we do not restrict ourselves to the most commonly used MIA. Instead, we calculate all Wilson coefficients relevant for a given process in the mass eigenstate approach, taking into account the full set of contributions - SM, Higgs, chargino, neutralino and gluino sectors. Further, we compare experimental results with the full 1-loop SUSY expressions, not just the dominant (usually gluino) term.

- To complete the bounds coming from the low-energy data, we also compare lower

mass bounds for SUSY particles, obtained from accelerator experiments, with the tree-level eigenvalues of the MSSM mass matrices.

For comparing theoretical predictions for the low-energy observables with experiment, we apply the following procedure. For a given set of SUSY parameters, we calculate all appropriate parton-level diagrams. Next, we construct expressions for the considered quantities using the central values of the QCD evolution factors and necessary hadronic matrix elements, obtained by perturbative SM and lattice-QCD computations, respectively. Finally, for every quantity Q we require:

$$|Q^{exp} - Q^{th}| \leq 3\Delta Q^{exp} + q|Q^{th}|, \qquad q = 0.5 \tag{3.2}$$

with the exception of ΔM_s, for which we require $(1+q)|Q^{th}| \geq Q^{exp}$.

The first term on the RHS of (3.2) represents the 3σ experimental error. The second term corresponds to the theoretical error. In principle, such an error differs from quantity to quantity and is usually smaller than $q = 50\%$, which we assumed as a generic number in all calculations. However, apart from the theoretical errors coming from uncertainities in the QCD evolution and hadronic matrix elements calculations, one should take into account also problems arising due to the limited numerical scan density. In principle, with a very dense scan, it should be possible to find SUSY parameters fulfilling (3.2) within the "true" theoretical errors of present calculations. Such a dense scan requires, however, a huge amount of computer time - with 16 or more free parameters and rather complicated mass eigenstate formulae, it would take months of CPU time. This does not seem to be necessary and may even be undesirable. Our goal is to find "generic" allowed values for the $K \to \pi\nu\bar{\nu}$ decay rates, i.e. values possible to obtain for fairly wide ranges of SUSY parameters, without strong fine-tuning and resorting to some very particular points of the parameter space where the experimental bounds are satisfied due to precise cancellations of various types of contributions. Thus, in our scan we use wide "theoretical" errors, assuming that this procedure points to the correct ranges of the MSSM parameters, and if necessary the exact values of such parameters fulfilling the bound in (3.2) with smaller q could always (or at least almost always) be found. This could be achieved e.g. by a denser scan or by more advanced numerical routines, possibly even solving numerically the set of non-linear equations given by all constraints.

The only exception from the procedure described above is the imposition of the constraint from the CP asymmetry $a_{\psi K_S}(t)$. Making the safe assumption that the supersymmetric contributions to the decay amplitude can be neglected, this asymmetry measures the phase of the $B_d^0 - \bar{B}_d^0$ amplitude

$$M_{12} = \langle B_d^0 | H_{eff}(\Delta B = 2) | \bar{B}_d^0 \rangle = |M_{12}| e^{i2(\beta + \theta_d)} \tag{3.3}$$

through

$$a_{\psi K_S}(t) = -a_{\psi K_S} \sin(\Delta M_d t) = \sin 2(\beta + \theta_d) \sin(\Delta M_d t) \ . \tag{3.4}$$

Here $-\beta$ is the phase of V_{td}, while θ_d is the new effective phase coming from the supersymmetric contributions. As in the general MSSM the presence of non-vanishing sfermion mass insertions implies contributions of several local operators to M_{12}, the phase θ_d suffers from potential uncertainities related to the hadronic matrix elements of these operators.

Only if one of these operators dominates over the others in the full amplitude can θ_d be cleanly related to supersymmetric parameters. In other cases its error can be sometimes very large and moreover is hard to estimate – it would require additional scanning over hadronic uncertainities for each given set of SUSY parameters. To avoid such problems, in our analysis we assume conservatively

$$|a^{exp}_{\psi K_S} - \sin 2(\beta + \theta_d)| \leq 2\Delta a^{exp}_{\psi K_S} \tag{3.5}$$

with $\sin 2(\beta + \theta_d)$ calculated in the MSSM for central values of the hadronic parameters and $a^{exp}_{\psi K_S} = 0.736 \pm 0.049$. Expressing everything in degrees we require then

$$|23.7^\circ - (\beta + \theta_d)| \leq 4.2^\circ. \tag{3.6}$$

Assuming only experimental and no theoretical errors on the R.H.S. of (3.5), we reject some otherwise valid points from our scan, but we checked that this does not have any significant effect on the results discussed in following sections.

Apart form the experimental bounds, there are also bounds from the requirement that the vacuum is stable, or that the true ground state of the theory does not break color and charge. We apply the corresponding Charge and Color Breaking (CCB) and unbounded from below MSSM scalar potential (UFB) bounds [43], which give constraints on the A-terms and consequently on the left-right elements of the sfermion mass matrices. We use the tree-level expressions in the form:

$$\begin{aligned}
|A_u^{IJ}|^2 &\leq (1 + 2\delta^{IJ}) f |Y_u^{max(I,J)}|^2 \left[(m_Q^2)^{II} + (m_U^2)^{JJ} + m_{H_2}^2 + |\mu|^2 \right], \\
|A_d^{IJ}|^2 &\leq (1 + 2\delta^{IJ}) f |Y_d^{max(I,J)}|^2 \left[(m_Q^2)^{II} + (m_D^2)^{JJ} + m_{H_1}^2 + |\mu|^2 \right], \\
|A_l^{IJ}|^2 &\leq (1 + 2\delta^{IJ}) f |Y_l^{max(I,J)}|^2 \left[(m_L^2)^{II} + (m_E^2)^{JJ} + m_{H_1}^2 + |\mu|^2 \right],
\end{aligned} \tag{3.7}$$

$$\begin{aligned}
|A_u^{IJ}|^2 &\leq f |Y_u^{max(I,J)}|^2 \left[(m_Q^2)^{II} + (m_U^2)^{JJ} + (m_L^2)^{KK} + (m_E^2)^{KK} \right], \\
|A_d^{IJ}|^2 &\leq f |Y_d^{max(I,J)}|^2 \left[(m_Q^2)^{II} + (m_D^2)^{JJ} + (m_L^2)^{KK} \right], \qquad I \neq J,\ K \neq I, J, \\
|A_l^{IJ}|^2 &\leq f |Y_l^{max(I,J)}|^2 \left[(m_L^2)^{II} + (m_E^2)^{JJ} + (m_L^2)^{KK} \right].
\end{aligned} \tag{3.8}$$

As suggested in some papers (see e.g. [44] for a comprehensive discussion), tree-level CCB/UFB bounds may not be very stable against radiative corrections. Again, we do not try to use more elaborate formulae, but relax the tree-level bounds by adding factors $f = 2$ on the RHS of all equations in (3.7) and (3.8). (Strict tree-level bounds correspond to $f = 1$.)

3.3 The adaptive scan algorithm

The numerical analysis laid out in the previous subsections requires us to scan an N-dimensional ($N \geq 16$) parameter space sufficiently densely to account for all regions where the quantity X of (2.5) possibly is large. A straightforward approach is to scan over a uniform N-dimensional grid. However, this is both time-consuming and ineffective. Nevertheless, we have performed some test scans of this kind to get a first notion of the

attainable rates of both branching ratios considered, as well as of X. We generated about 1.6M points, only about 1% of which passed all theoretical and experimental constraints. The distribution of the remaining points is shown in Fig. 2. What can be observed is that most points are close to the SM value of X, i.e. new-physics effects are very small for most grid points. The departure from the SM lies along straight lines, which is an obvious artifact of the small grid density, in spite of the fact that more than 1 million points were generated.

However, what we are interested in is not so much the somewhat vague notion of a "probability density" for quantities shown in various scatter plots, which is clearly a function of the choice of parameters, of their scaling chosen during the scan (e.g. linear or logarithmic) and the range considered for each parameter. Rather, we are interested in the maximal allowed regions of the parameter space and the extremal values of the observables, viz. the (complex) function X, which are physical (i.e. parameterization-invariant). To find this information, a dense and very time-consuming scan is necessary.

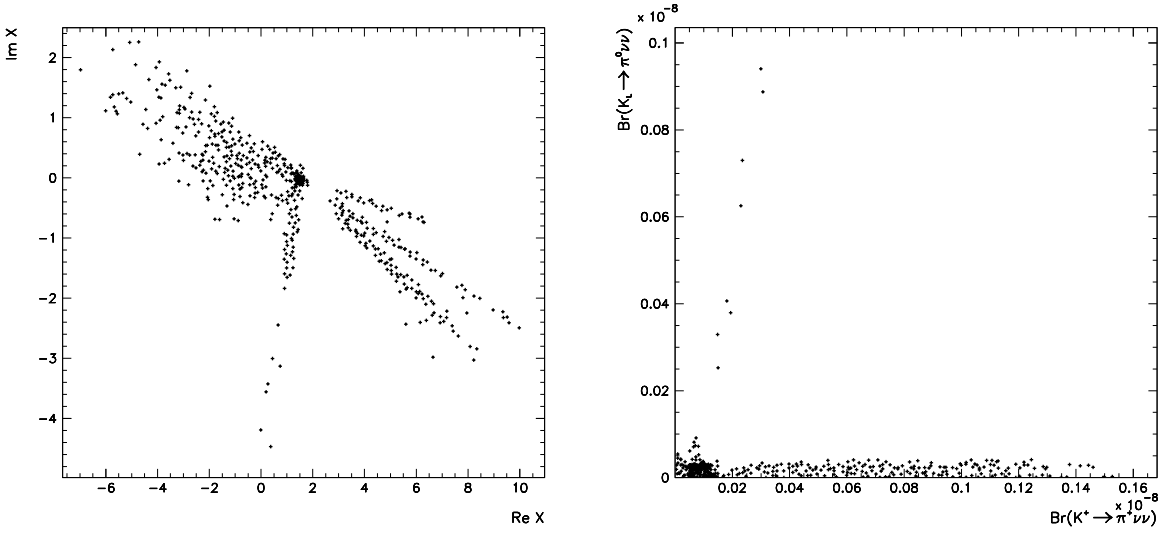

Figure 2: Scatter plot of X, $Br(K^+ \to \pi^+\nu\bar{\nu})$ and $Br(K_L \to \pi^0\nu\bar{\nu})$ distributions for $\tan\beta = 2$ and uniform grid scan. Parameters varied in the ranges $0 \le \gamma \le 180°$, $200 \le M_{sq} \le 500$, $150 \le M_{sl} \le 300$, $-400 \le \mu \le 400$, $200 \le M_2 \le 600$, $150 \le M_A \le 300$, $-1 \le A \le 1$, mass insertions between 0.003 and 0.3, their phases set to 0°, 45° or 90°.

In practice, due to the number of free parameters, the grid involves only 2 to 5 different values for each parameter, posing an additional risk that a relevant region of the parameter space may fall through the grid altogether. In fact, this will be likely if the largest effects do not simply occur where some parameters are smallest and others are largest, but in areas where some type of cancellation, even moderate, is needed to fulfill the experimental constraints.

A random generation of parameter points may exhibit some of these overlooked regions. Such an approach is particularly useful when, as it is true for the quantities considered in

this paper, the analyzed expressions depend strongly only on a subset of M free parameters, $M < N$. In this case one can think in terms of an "effective density" – the projection of the random points onto the M-dimensional subspace of "relevant" parameters now has a density (in that subspace) that is about $(2 \ldots 5)^{N/M}$ times higher than for a uniform grid. To see this, envision projecting the original grid: for given relevant parameters, the remaining $N - M$ parameters describing a given point, which are approximately irrelevant, just parameterize points projected onto the same M-dimensional point. Thus in the uniform-grid approach one repeats the same analysis many times. Conversely, the projection of the randomly distributed points is again randomly distributed over the subspace, and each new point gives additional information.

Note that in general the subset of relevant parameters is different for each observable. This precludes just removing the irrelevant parameters from the scan, in the case one believes to know them beforehand. The random scan, on the other hand, gives an improved effective density for each of the corresponding subspaces.

Still, for randomly distributed parameter points, an expression $|X - X^{SM}|$ describing the deviation from the SM prediction (or similar expressions for other observables, which we use to constrain the parameter space) will give a small number over most of the parameter space. On the other hand, in the regions where it is large it also tends to vary more strongly. Therefore, while effectively improving the grid density, random generation of points with a uniform distribution may still miss the exact maxima for realistic numbers of points. It would be desirable to generate points more densely where the function X is large and/or varies quickly - such a procedure would be particularly efficient if, as is expected, our results mainly depend on just a few parameters.

Recently, Brein [39] has suggested using an adaptive Monte-Carlo integration algorithm such as VEGAS [40] for a similar purpose. VEGAS performs "importance sampling" via an iterative algorithm. At each iteration, it generates a certain number of points according to a probability distribution determined by the integrand values encountered during the previous iterations. The probability distribution is chosen to be separable and is adjusted after each iteration. The initial distribution is chosen to be uniform. This procedure is designed to minimize the statistical error of the integration by increasing the number of points in those parts of the integration volume where the integrand is found to be large. While we are not interested in computing any integral to any given precision, VEGAS does provide what we desire, if we choose our integration volume as the parameter space (suitably rescaled) and the integrand such that it becomes large for large values of X. We found the following "integrand" useful:

$$f = \begin{cases} 0 & \text{parameter set rejected by constraints} \\ \left|X - X^{SM}\right|^n & \text{constraints satisfied} \end{cases} \tag{3.9}$$

where X is the quantity defined in (2.5), X^{SM} is its SM central value (2.4) and we varied the power n between 3 and 8. (We do not write explicitly the dependence of X on γ and SUSY parameters.) We "integrated" this function numerically with the VEGAS routine, storing all generated Monte Carlo points in a separate file along with the values of various observables for analysis. The parameter ranges used for the integration are given in Table 1.

Using the VEGAS algorithm has the great advantage of sampling mostly the important regions of parameter space, where the function X really depends significantly on at least

some of the parameters. It also allows us to increase safely the number of the degrees of freedom— adding new variables has only a moderate effect on total computation time as long as the function X, or in general the VEGAS integrand, is weakly dependent on them. In fact, we were able to perform Monte Carlo sampling over huge portions of the MSSM parameter space, probably never tried before, of up to 63 dimensions (parameters), and to judge only afterwards, from the obtained distributions, which of the parameters where important for a given problem.

The applied procedure carries some dangers. First, one should mention a point that is not always appreciated. As is well known, the "random" numbers provided by various standard libraries are in fact deterministic sequences which may or may not satisfy certain conditions of randomness, or absence of correlation. In our context, when one uses N subsequent numbers in the sequence to define a point in an N-dimensional parameter space, the widely used generators based on linear congruences tend to concentrate these points on a bundle of $(N-1)$-dimensional hyperplanes. This can reintroduce the danger of points of interest "falling through the grid" mentioned above. To address this problem, we used two different random number generators, both of which avoid such correlations. The first is a subtractive Mitchell-Moore generator discussed by Knuth [45] in an implementation of Kleiss [46]. The second is based on a combination of Fibonacci and arithmetic sequences proposed by [47] in an implementation of James [48]. We obtained similar plots for both algorithms, which strengthens our conviction that our procedure is stable and does not miss any relevant regions.

Also, there is the question of stability of data samples obtained in this way. In order to check it, we varied the power n in (3.9) in the range of 3 to 8, and inspected how the shape of the plotted regions evolved with the numbers of points generated. The choice of the particular function f appears to affect mostly the time in which the shape of various distributions stabilizes, not the boundaries itself. Similar comments apply to tuning of the internal control parameters of the VEGAS routine.

4 Results

4.1 Sensitivity to scan parameters

As a first step of our analysis, we plotted distributions of $|X|$ obtained in the "constrained" scan (described in detail in Section 3.1) versus various flavour diagonal and off-diagonal parameters, in order to check the sensitivity of the considered decay rates to them. The plots obtained support our conjecture that only a modest subset of the MSSM parameters is in the first approximation relevant for our analysis, even after including the complicated set of additional bounds. Most of the obtained distributions for flavour diagonal parameters are flat (dependence on M_A, M_1, $m_{\tilde{g}}$) or almost flat (dependence on M_{sl}, A). A more pronounced dependence could be observed only in the case of γ and the SUSY parameters plotted in Fig. 3.

The dependence visible for the other parameters can be explained by looking at Fig. 4, where we plotted the contributions from the chargino and neutralino sectors to $\lambda_t X$. The chargino diagrams are always strongly dominant, typically one order of magnitude larger than the neutralino contributions. Gluino exchanges (in our case penguin diagrams

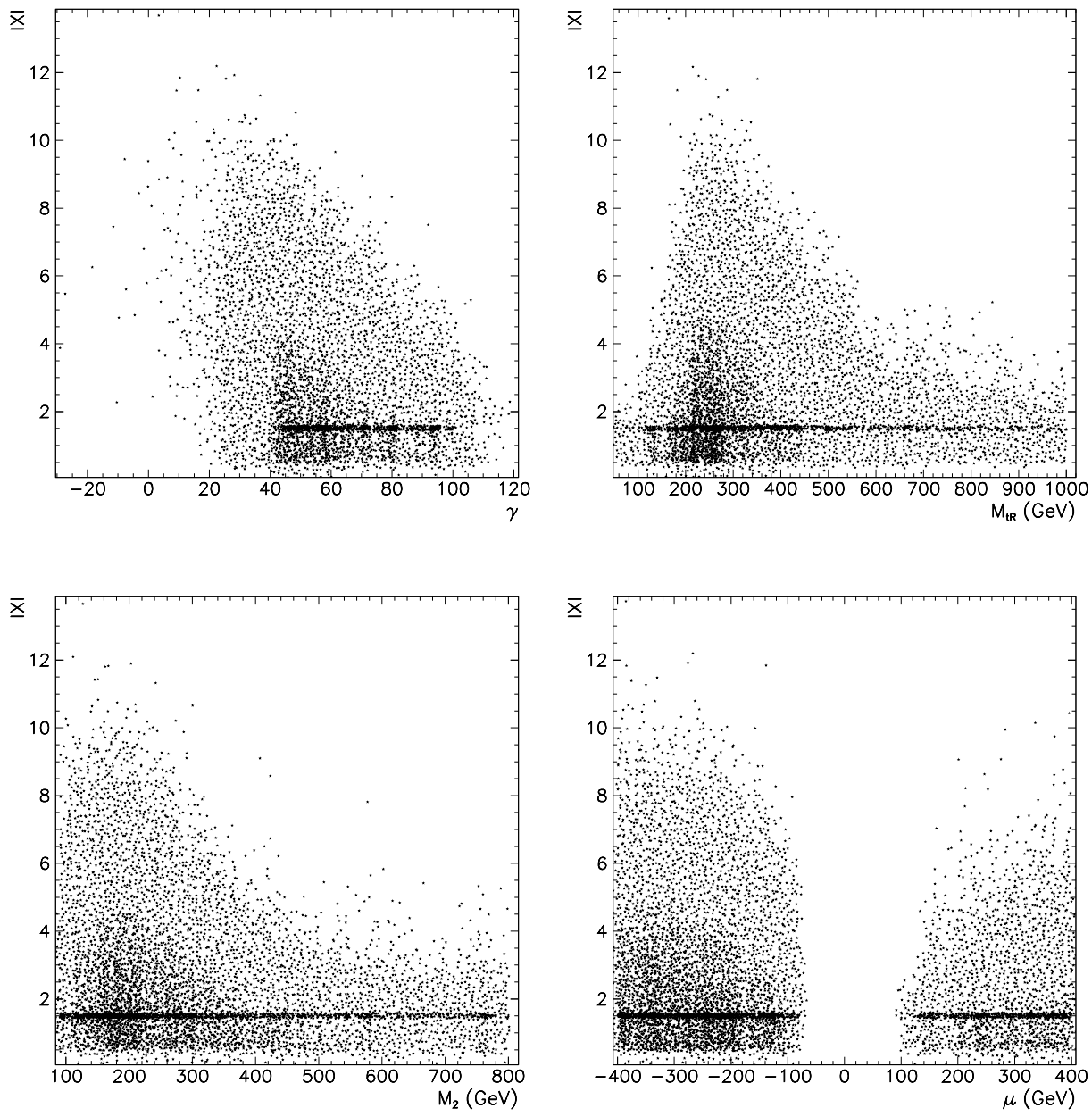

Figure 3: Distributions of X versus γ, $M_{\tilde{t}_R}$, M_2 and μ for $\tan\beta = 2$ in data set generated during VEGAS integration.

only) can be always completely neglected, as we checked that they are several orders of magnitude smaller than other contributions. Thus, the size of both decay rates, $Br(K^+ \to \pi^+\nu\bar{\nu})$ and $Br(K_L \to \pi^0\nu\bar{\nu})$, is determined by the chargino-up-squark contribution and should depend mostly on the parameters entering the expression for this amplitude, in agreement with the results of [12, 30, 32]. This is not true for the variety of experimental and theoretical bounds we took into account in constraining the MSSM parameter space – they also depend on other parameters (e.g., the hole in the μ distribution comes of course from the bounds on the lightest neutralino and chargino masses). This has some secondary influence on the shape of the plots in Fig. 3, as the imposed constraints can lead to correlation between the allowed ranges of some of the parameters directly relevant for the $K \to \pi\nu\bar{\nu}$ decay calculation. For instance, attainable values of $|X|$ grow first with MSSM masses like $M_{\tilde{t}_R}$ or M_2, because experimental constraints for squark mass insertions are easier to satisfy for heavier SUSY particles (similarly for distributions with $M_{\tilde{t}_L}$ or M_{sq}, not included in Fig. 3). Later they go down again because the suppression of SUSY loop diagrams contributing to $K \to \pi\nu\bar{\nu}$ decays for heavy virtual particles dominates above the effect of weakening the impact of the experimental constraints. One should also note that the distribution of γ in Fig. 3 shows an increased density of points around SM-preferred value $\gamma \approx 70^\circ \pm 30^\circ$ – for the remaining points, the larger or smaller value of the KM phase must be compensated by the phases of some mass insertions.

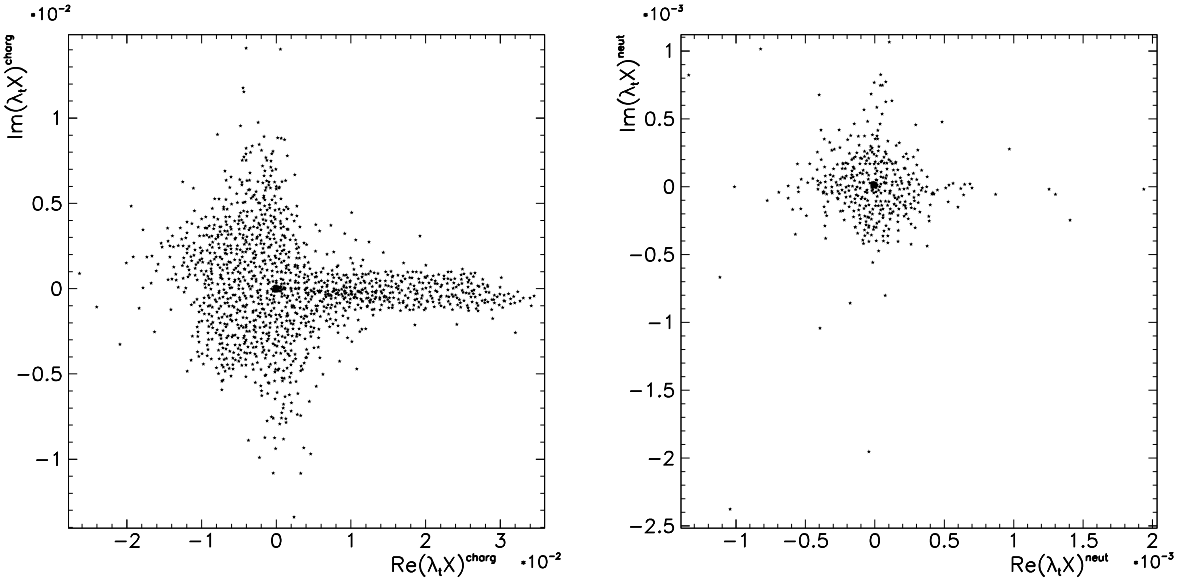

Figure 4: Chargino and neutralino contributions to $\lambda_t X$ for $\tan\beta = 2$.

An interesting observation can be made by comparing the relative size of penguin- and box-type contributions to the $K \to \pi\nu\bar{\nu}$ decay amplitude. A common assumption used in the literature says that box diagrams are parameterically suppressed by $\mathcal{O}(M_W^2/M_{slepton}^2)$ and can be safely neglected when compared with Z^0-penguin contribution. This is certainly not justified for light slepton masses, and not very accurate even for moderate $M_{sl} \sim 300$ GeV. In Fig. 5 we plot the absolute value of the ratio of box to penguin contribution against the slepton mass, including in the distribution only particularly interesting

points for which the $K^+ \to \pi^+\nu\bar{\nu}$ decay rate is large, $Br(K^+ \to \pi^+\nu\bar{\nu}) \geq 1.5 \cdot 10^{-10}$. As can be immediately seen, for slepton masses just above 100 GeV box and penguin contributions are in a substantial number of cases comparable in amplitude, and even for $M_{sl} = 300$ GeV their ratio can still reach 30%. Thus box diagrams definitely should be taken into account in realistic calculations. Of course, their presence introduces slepton mass dependence into the considered branching ratios, which would otherwise be negligible.

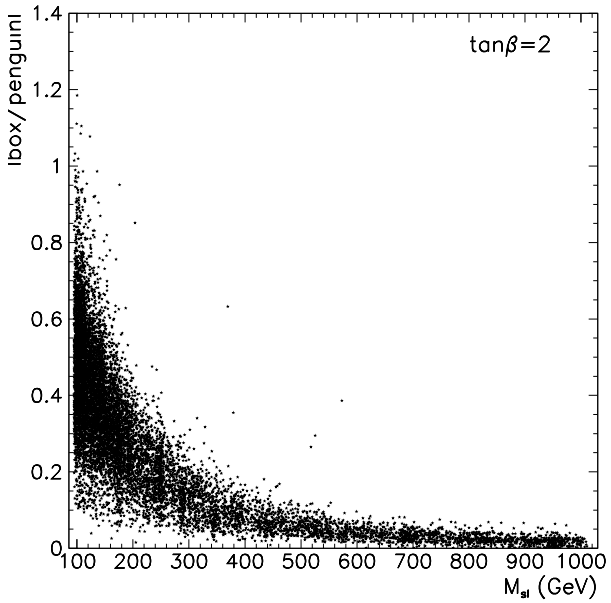

Figure 5: Absolute value of the ratio of box to penguin contributions as a function of slepton mass for $\tan\beta = 2$. Only points for which $Br(K^+ \to \pi^+\nu\bar{\nu}) \geq 1.5 \cdot 10^{-10}$ are plotted.

In our "constrained" scan we varied 3 types of mass insertions, δ^{12}_{LL}, δ^{13}_{ULR} and $\delta^{23\star}_{ULR}$. We checked that the dependence on δ^{12}_{LL} is actually almost negligible, as expected because it is strongly constrained by bounds coming from ϵ_K and ΔM_K measurements: $\delta^{12}_{LL} \leq 0.05$. In Fig. 6 we plot the dependence on the moduli of the remaining two ULR mass insertions. The dependence on them is quite pronounced, in agreement with the conclusions of [30] that the second order ULR terms in the MI expansion give the dominant contribution to the considered decays. We return to this point in Subsect. 4.3 below. For comparison, we also plot $|X|$ against just the real part of δ^{13}_{ULR}, which exhibits less correlation.

4.2 Allowed ranges for the X function, $Br(K_L \to \pi^0\nu\bar{\nu})$ and $Br(K^+ \to \pi^+\nu\bar{\nu})$

The most interesting information from scanning over SUSY parameters are the maximal values of $|X|$, θ_X and the branching ratios $Br(K_L \to \pi^0\nu\bar{\nu})$, $Br(K^+ \to \pi^+\nu\bar{\nu})$ which can

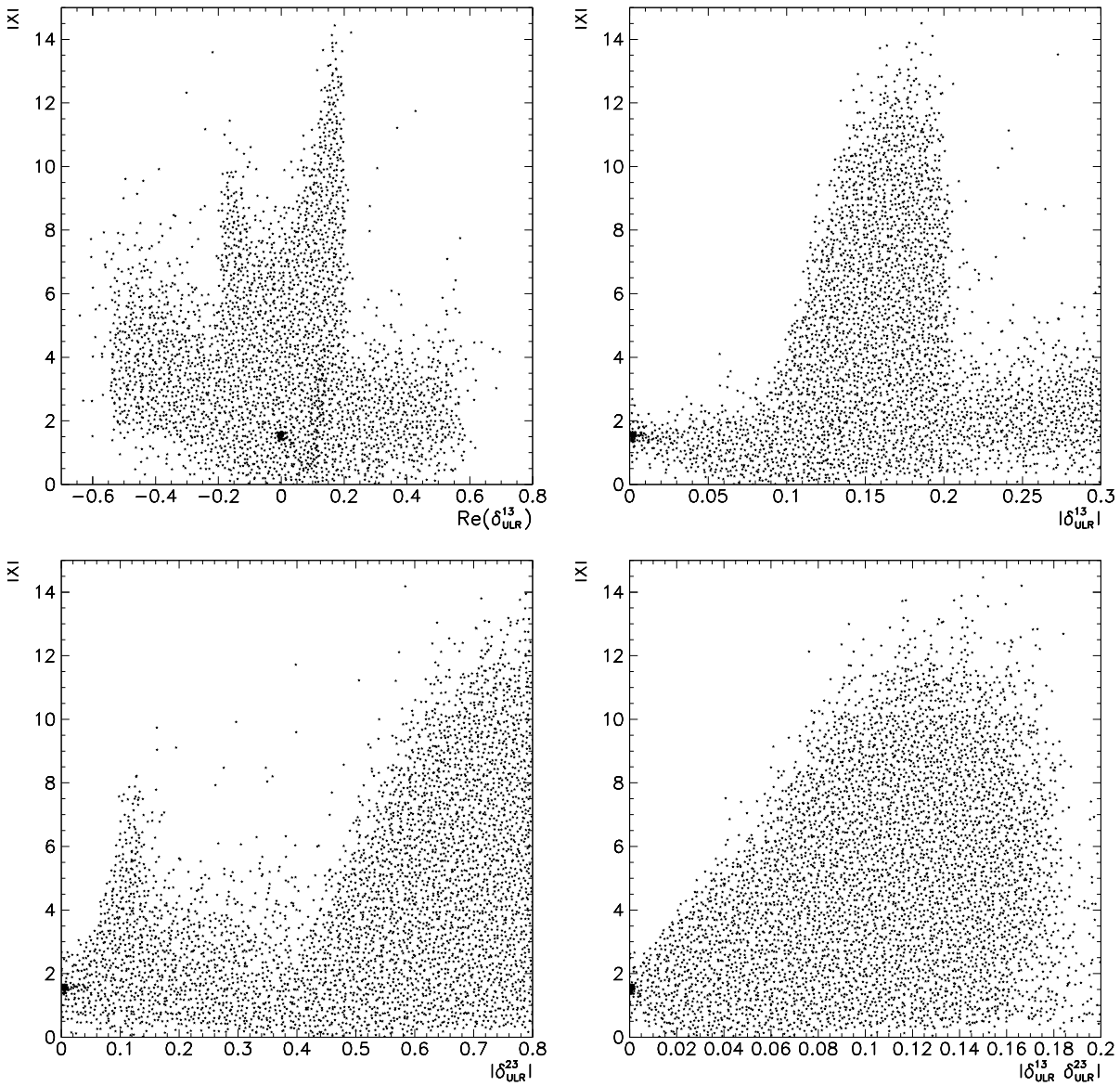

Figure 6: Distributions of X versus real part and modulus of δ_{ULR} mass insertions for $\tan\beta = 2$. These plots have been produced using the exact results given in the Appendix and not the MIA.

be obtained taking into account the bounds given by other processes. In Fig. 7 we plot distributions of those quantities for $\tan\beta = 2$.

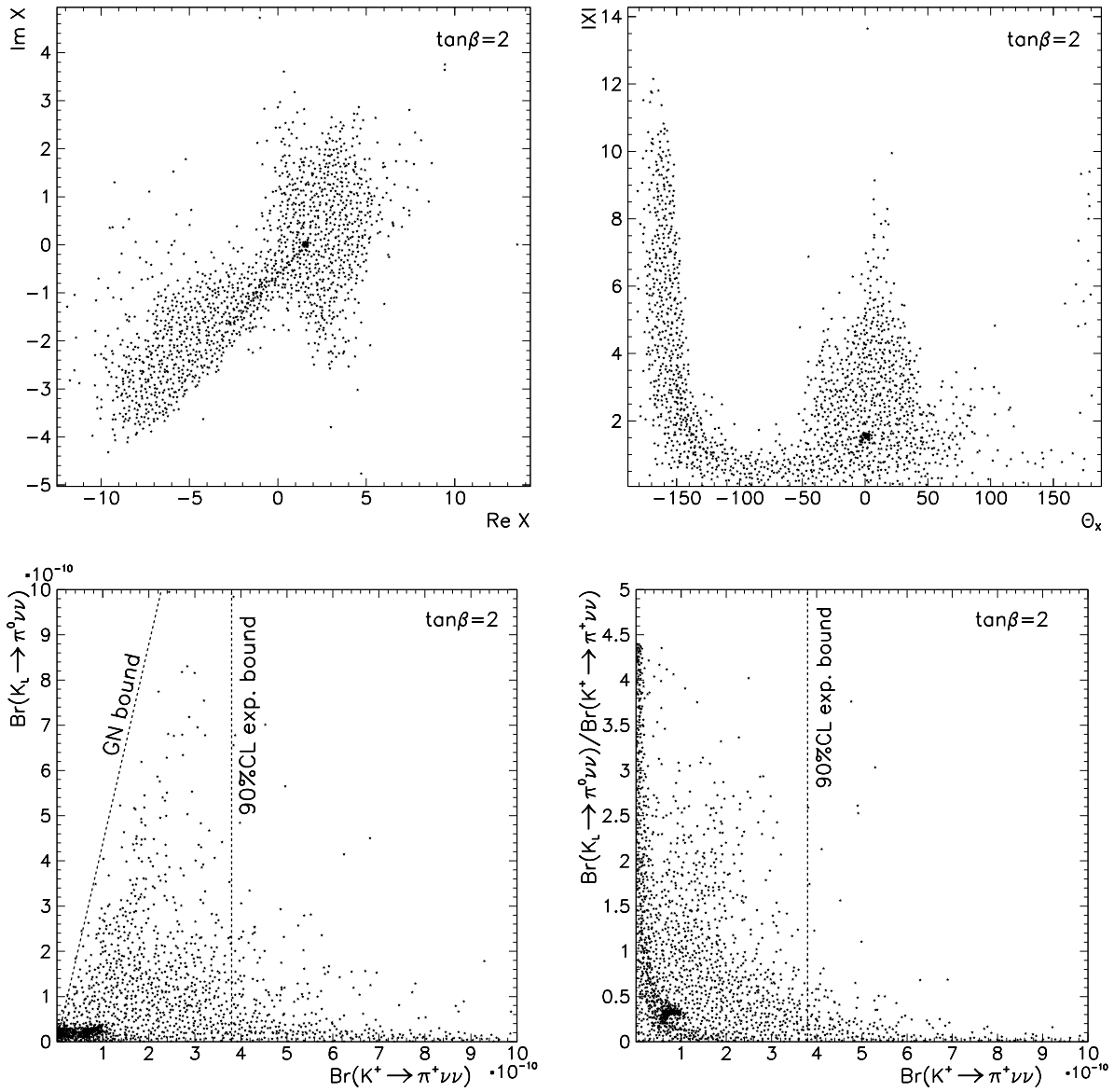

Figure 7: Distributions of X and $Br(K_L \to \pi^0\nu\bar{\nu})$, $Br(K^+ \to \pi^+\nu\bar{\nu})$ for $\tan\beta = 2$.

As can be seen from Fig. 7, the allowed values for $Br(K_L \to \pi^0\nu\bar{\nu})$ and $Br(K^+ \to \pi^+\nu\bar{\nu})$ can be significantly enhanced compared to the SM prediction, even by an order of magnitude. Such large values are higher than the 90%CL experimental bound [19], $Br(K^+ \to \pi^+\nu\bar{\nu}) < 3.8 \cdot 10^{-10}$, therefore this decay can already be used to constrain the MSSM parameter space. We will analyze this elsewhere. One should note that the obtained values for the branching ratios do not violate the Grossman-Nir (GN) [26] bound $Br(K_L \to \pi^0\nu\bar{\nu})/Br(K^+ \to \pi^+\nu\bar{\nu}) \leq 4.4$, which can be regarded as a simple cross-check of the correctness of our numerical codes.

In Fig. 8 we plot the allowed range of X after imposing the cut [19] $Br(K^+ \to$

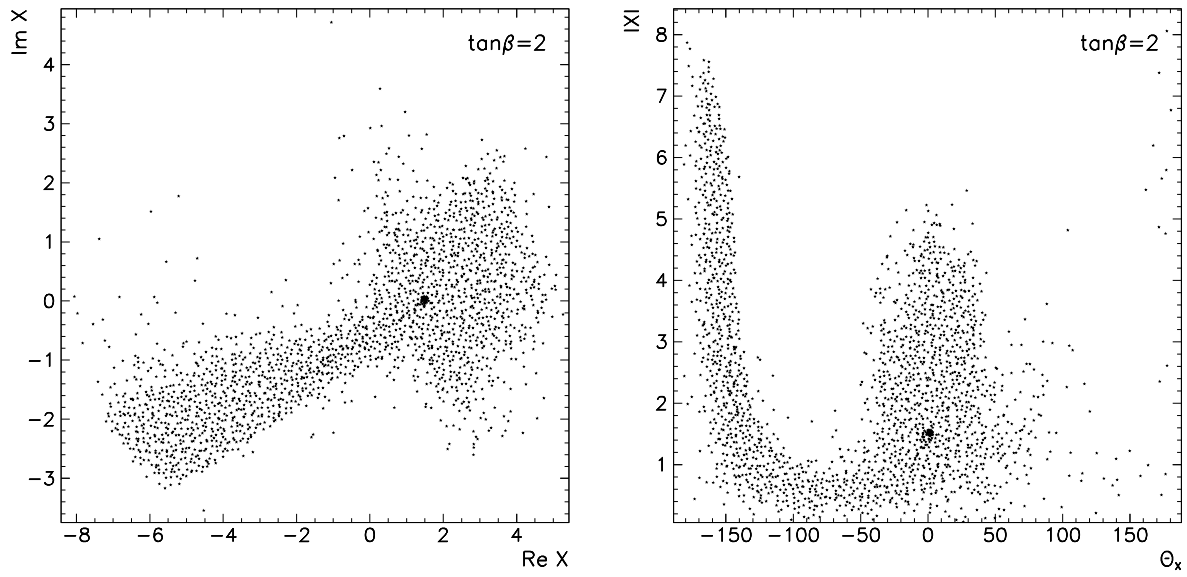

Figure 8: Distributions of X for $\tan\beta = 2$ after imposing constraint $Br(K^+ \to \pi^+\nu\bar{\nu}) < 3.8 \cdot 10^{-10}$.

$\pi^+\nu\bar{\nu}) < 3.8 \cdot 10^{-10}$. Even with this constraint, $|X|$ could be several times bigger than the SM value (2.4). Also, its phase can still vary almost freely, however is preferred to be in a broad range $-160° \leq \theta_X \leq 70°$. Such a freedom leads to a possible enhancement of the ratio $Br(K_L \to \pi^0\nu\bar{\nu})/Br(K^+ \to \pi^+\nu\bar{\nu})$ even for large values of $Br(K^+ \to \pi^+\nu\bar{\nu})$, as can be observed in Fig. 7.

The plots of X in Figs. 7 and 8 display a conspicuous correlation between the phase and modulus. This can be understood from the allowed region in the complex plane for the chargino contribution to $\lambda_t X$ shown in Fig. 4. The experimental constraints we apply constrain its imaginary part to be relatively small, especially when the real part becomes large. Taken together with the fact that $\mathrm{Re}\lambda_t < 0$ (any γ) and that γ is sufficiently constrained (cf. Fig. 3) to always imply $\mathrm{Im}\lambda_t > 0$, this explains the shape of the allowed region in the complex X plane.

Finally, in Fig. 9 we plot distributions of $Br(K_L \to \pi^0\nu\bar{\nu})$ and $Br(K^+ \to \pi^+\nu\bar{\nu})$ for higher value of $\tan\beta = 20$. Results are qualitatively similar to those obtained for $\tan\beta = 2$, however for larger $\tan\beta$ (particularly $\tan\beta \geq 10$) it is easier to generate parameters sets giving high branching ratios (or their ratio).

To better illustrate the effects shown in the figures in this section, we give in Table 3 specific examples of MSSM parameter choices leading to particularly interesting results. The quotation marks on some quantities in this table indicate that in evaluating these quantities we have set hadronic parameters to their central values as discussed in Subsection 3.2. Varying these parameters, it is easy to reproduce the relevant experimental data within one standard deviation.

Parameter	Example 1	Example 2
$\tan\beta$	2	20
M_A	333	260
μ	-375	-344
$M_{\tilde{g}}$	437	928
M_2	181	750
M_{sq}	308	608
$M_{\tilde{t}_L}$	138	215
$M_{\tilde{t}_R}$	279	338
M_{sl}	105	884
A	-0.289	-0.342
γ	64°	38°
δ^{12}_{LL}	$(2.18 - 5.02i) \cdot 10^{-5}$	$(7.57 - 0.871i) \cdot 10^{-4}$
δ^{13}_{ULR}	$(-1.52 + 0.748i) \cdot 10^{-4}$	$0.292 - 0.213i$
$\delta^{23\star}_{ULR}$	$0.001 - 0.604i$	$0.239 - 0.195i$
"$\lvert\varepsilon_K\rvert$"	$2.35 \cdot 10^{-3}$	$2.10 \cdot 10^{-3}$
"ΔM_d"	$3.15 \cdot 10^{-13}$	$2.55 \cdot 10^{-13}$
"ΔM_s"	$1.03 \cdot 10^{-11}$	$1.19 \cdot 10^{-11}$
"$Br(B \to X_s\gamma)$"	$3.88 \cdot 10^{-4}$	$3.93 \cdot 10^{-4}$
$Br(K^+ \to \pi^+\nu\bar{\nu})$	$1.78 \cdot 10^{-10}$	$2.07 \cdot 10^{-10}$
$Br(K_{\rm L} \to \pi^0\nu\bar{\nu})$	$3.08 \cdot 10^{-11}$	$4.34 \cdot 10^{-10}$

Table 3: Examples of MSSM parameter points passing experimental constraints at the assumed accuracy (see discussion in section 3.2) and giving enhanced $K^+ \to \pi^+\nu\bar{\nu}$ and $K_{\rm L} \to \pi^0\nu\bar{\nu}$ decay rates. Units are as in Table 1. See text for the meaning of quotation marks.

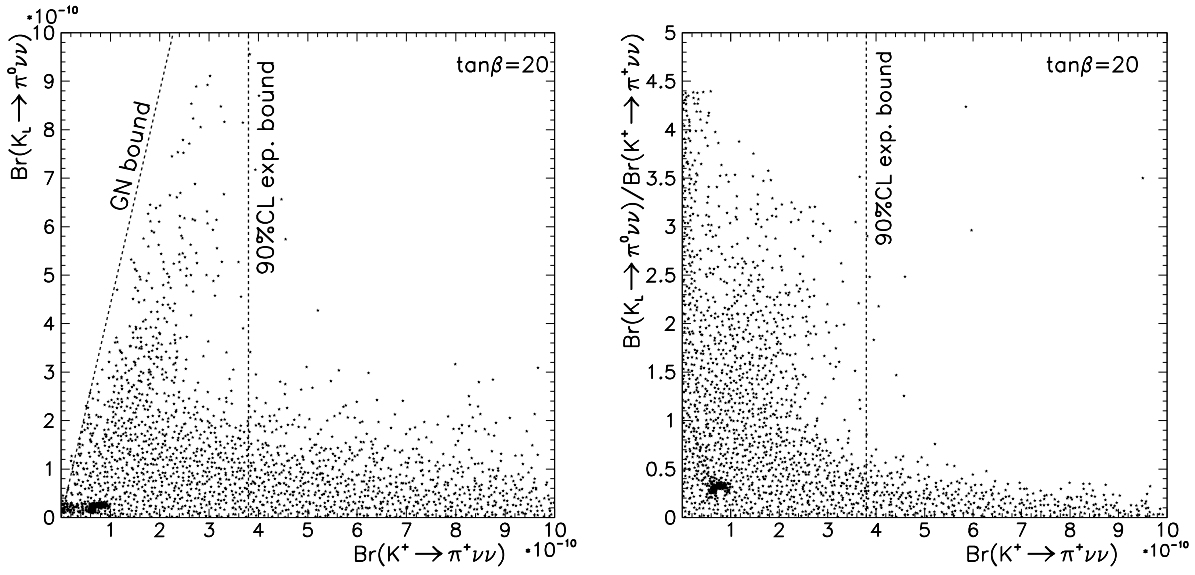

Figure 9: Distributions of $Br(K_L \to \pi^0 \nu\bar{\nu})$ and $Br(K^+ \to \pi^+ \nu\bar{\nu})$ for $\tan\beta = 20$.

4.3 Comparison with earlier literature

Colangelo and Isidori [30], extending and clarifying earlier work [38, 12], have used the fact that all contributions to the Z^0-penguin must be at least of second order in the VEV by gauge invariance to trace the dominant SUSY contribution, at least in the case of large X, to the following term, which can be obtained as part of the chargino contribution (A.14) to the Z^0-penguin:

$$\left[P_L^{c(0)}\right]_{JI} = -\frac{1}{8} V_{RI} V_{SJ}^* Z_U^{Rk*} Z_U^{(N+3)k} Z_U^{(N+3)i*} Z_U^{Si} Z_+^{1m} Z_+^{1m*} C_2(m_{C_m}^2, m_{U_k}^2, m_{U_i}^2). \tag{4.1}$$

In the mass insertion approximation, this term contributes only starting from the second order, where it is proportional to the product $\delta^{13}_{ULR}\delta^{23*}_{ULR}$.

Fig. 6 is consistent with this observation [30], as is evidenced by the triangular excluded region in the bottom-right plot in that figure: $|X|$ is only large when also $|\delta^{13}_{ULR}\delta^{23*}_{ULR}|$ is large.

In fact, together with the large box contributions we reported in Subsect. 4.1 and Fig. 5, this plot suggests that even the box contributions, which were found to be subleading in [30] and earlier in [38], follow the same pattern, a point that has so far not been made in the literature. Indeed, there is no reason why the box diagram should not be competitive with the up-squark-chargino contribution to the Z^0-penguin for light slepton mass. The chargino-box contribution (A.7), ignoring slepton flavour violation and charged-lepton masses, contains a term

$$\begin{aligned} \left[B_L^{c(0)}\right]_{JIKL} &= -\frac{M_W^2}{2} \delta_{KL} V_{RI} V_{SJ}^* Z_U^{Rk*} Z_U^{Sk} Z_-^{1m} Z_-^{1n*} Z_+^{1m} Z_+^{1n*} \\ &\times m_{C_m} m_{C_n} D_0(m_{C_m}^2, m_{C_n}^2, m_{U_k}^2, m_{L_L}^2), \end{aligned} \tag{4.2}$$

which is quite similar to (4.1). Consequently, it receives a similar second-order contribution in the mass insertion approximation, in contrast to the finding in [30] that the

box diagrams contribute only at the level of three off-diagonal mass insertions. The double squark left-right flip is again the most important mixing parameter, even though no $SU(2)$-breaking powers of the VEV are required, unlike the case of the Z^0-penguin. For the chargino contribution, that requirement therefore turns out to be a red herring, although it still explains why gluino and neutralino-penguin contributions are small. All large effects are proportional to the double up-squark left-right mixings simply because these are weakly constrained and at the same time avoid the double CKM suppression, both of which facts were correctly stated by the authors of [30].

More stringent bounds on the left-right mass insertions than those used in this work have been derived in [32] from a general MSSM RG analysis, however their results depend on the assumption that the soft-breaking terms are present already at the GUT scale. This is a model-dependent assumption, not necessarily true in the general MSSM. There are also potentially dangerous contributions from double mass insertions to $\Delta S = 2$ processes that might lead to a violation of bounds from $K^0 - \bar{K}^0$ mixing. These are automatically taken into account in our computation by our exact diagonalization of the squark mass matrices.

4.4 Extended scan over MSSM parameters

The "adaptive scan" method [39] desribed in Section 3.3 allows for efficient exploration of really huge multi-dimensional parameter spaces, especially when the dependence of the analyzed results on most of those parameters is not very strong. Therefore, we tried to check how our results change if we get rid of virtually all assumptions usually used to relate MSSM parameters and treat them all as free independent quantities. We varied randomly the following quanties:

- the angle γ (real)
- CP-odd Higgs mass M_A (real)
- $U(1)$ gaugino mass M_1 (complex)
- $SU(2)$ gaugino mass M_2 (complex)
- gluino mass $m_{\tilde{g}}$ (real)
- μ parameter (complex)
- diagonal left slepton mass m_L^2, common for all generations (real)
- diagonal right slepton mass m_R^2, common for all generations (real)
- 9 independent diagonal mass parameters in squark mass matrices, 3 parameters for each of left, up-right and down-right mass matrix (all real)
- common sfermion LR mixing parameter A (real)
- 3 independent LL mass insertions in squark mass matrices: δ^{12}_{LL}, δ^{13}_{LL}, δ^{32}_{LL} (all complex)

- 6 independent RR mass insertions in squark mass matrices: δ^{12}_{DRR}, δ^{13}_{DRR}, δ^{32}_{DRR}, δ^{12}_{URR}, δ^{13}_{URR}, δ^{32}_{URR} (all complex)
- 12 independent LR up- and down-squark mass insertions δ^{12}_{DLR}, δ^{13}_{DLR}, δ^{32}_{DLR}, δ^{21}_{DLR}, δ^{31}_{DLR}, δ^{23}_{DLR}, δ^{12}_{ULR}, δ^{13}_{ULR}, δ^{32}_{ULR}, δ^{21}_{ULR}, δ^{31}_{ULR}, δ^{23}_{ULR} (all complex)

Altogether this gives 63 real degrees of freedom, more than half of the free parameters of the completely unconstrained (but R-parity-conserving) MSSM. For the SUSY mass parameters we use the same limits as given in Table 1, with the additional requirement $|M_1| \geq 20$ GeV; for new complex parameters we assume their phase to vary completely freely. Of course, for any parameter point we still apply all experimental and theoretical constraints listed in Section 3.2. Such an extensive scan was probably never reported before in the literature, so it is very interesting even to see if such a general MSSM version still retains any predictive power. The answer is positive – the results obtained for both analyzed decays, $K_L \to \pi^0\nu\bar{\nu}$ and $K^+ \to \pi^+\nu\bar{\nu}$, remain qualitatively similar to those already discussed for the "constrained" scan case!

Plots equivalent to those shown in Fig. 3 confirm the assumption that the dependence on most new parameters is weak (i.e. distributions are flat). Actually, in some cases like left stop and right sbottom mass parameters they become even flatter than in Fig. 3, as both discussed branching ratios do not depend directly on them (at least not strongly), and various experimental constraints can be satisfied varying additional parameters.

The allowed ranges for X and both branching ratios are extended somewhat in the 63-parameter scan, but not drastically, as illustrated in Fig. 10. In general, as could be expected, it is easier to generate a θ_X in the full range, there are more points with large $Br(K^+ \to \pi^+\nu\bar{\nu})$, $Br(K_{\rm L} \to \pi^0\nu\bar{\nu})$ or their ratio, but in general all distributions are still well defined in shape, just a bit broader. Thus, the most important conclusion of this kind of analysis is the statement that even the almost fully general low-energy MSSM does not lose its predictive power and exploring it can still lead to reasonable and well defined results. Although it requires more effort in numerical computation, it also minimizes the possibility of overlooking some interesting scenarios which can be realized for particular SUSY parameter choices.

The numerical analysis described in this section can also be used to put bounds on the allowed magnitude of the mass insertions in the squark sector, without resorting to the simplifying assumptions made in the traditional literature – absence of cancellations, neglect of interference of SM and SUSY contributions, the MIA. Results of such an analysis will be presented elsewhere.

5 Conclusions

In this paper we have analyzed the rare decays $K^+ \to \pi^+\nu\bar{\nu}$ and $K_{\rm L} \to \pi^0\nu\bar{\nu}$ in a general MSSM with conserved R-parity. Our analysis goes beyond those present in the literature in that

- we do not use the MIA but rather work in the mass eigenstate basis for all particles,

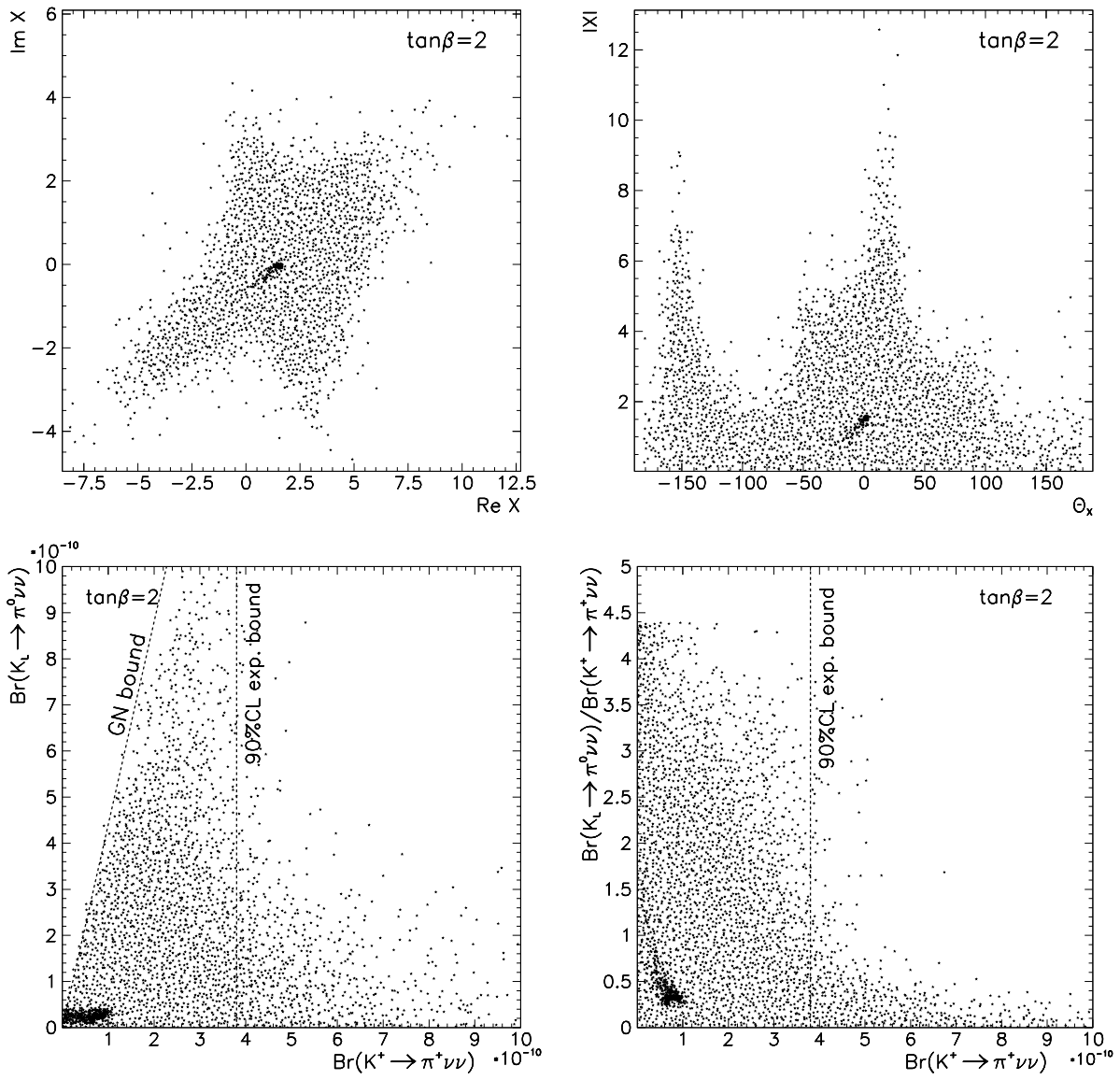

Figure 10: Distributions of X, $Br(K_L \to \pi^0 \nu\bar{\nu})$ and $Br(K^+ \to \pi^+ \nu\bar{\nu})$ for $\tan\beta = 2$ in the 63-parameter scan.

- we do not assume the dominance of certain contributions, as done frequently in the literature, thus allowing for cancellations and interferences of different diagrams contributing to the decay rates in question,

- we consider a scan of a very large space of parameters, 16 in the constrained scan and 63 in the extended scan, that to our knowledge has been presented here for the first time.

We should emphasize that the physics scenario considered here differs from the simple new physics scenario discussed in [15, 16] in that the new physics contributions to $K \to \pi\nu\bar{\nu}$ in the general MSSM do not only affect the function X as in [15, 16], but also modify the values of the CKM parameters. While the values of $|V_{us}|$, $|V_{ub}|$ and $|V_{cb}|$, measured in tree-level decays, are the same in both papers, the presence of relevant new phases in $B^0_{d,s} - \bar{B}^0_{d,s}$ mixings and ε_K in the general MSSM can significantly alter the values of γ, β and R_t that are used in the evaluation of the branching ratios for $K \to \pi\nu\bar{\nu}$. Consequently the comparison with the results presented in [16] has to be made with care. For instance the relation between β_X and θ_X in (2.23) can be modified in the general MSSM through the change of the angle β. While in [16] one has $\beta = (23.5 \pm 2.0)^\circ$, here one typically finds $12^\circ \leq \beta \leq 27^\circ$ but this modification can be compensated by a change of θ_X so that β_X remains unchanged.

More important then is the difference between R_t used in [16] and R_t found here. As $\gamma = (65 \pm 7)^\circ$ in [16] but $20^\circ \leq \gamma \leq 110^\circ$ here (see Fig. 3), the corresponding values of R_t obtained from (2.19) with $R_b = 0.37$ are $0.86 \leq R_t \leq 0.95$ and $0.66 \leq R_t \leq 1.18$, respectively.

While these differences in the CKM parameters play some role, they turn out to be subdominant in comparsison with the differences between the values for X used here and in [16]: compare (1.9) and Fig. 10.

Concerning individual contributions, in agreement with [12, 30, 32] we find that chargino diagrams are always strongly dominant, typically one order of magnitude larger than the neutralino contributions. Gluino exchanges are fully negligible. However, unlike these authors we find that in addition to chargino mediated Z^0-penguins, chargino box diagrams can be important and even dominant for light charged slepton masses. Thus from the point of view of the decay rates $Br(K^+ \to \pi^+\nu\bar{\nu})$ and $Br(K_L \to \pi^0\nu\bar{\nu})$, the general MSSM is a new physics scenario with enhanced Z^0-penguins carrying a new complex phase, similarly to what has been considered in [16]. However, the presence of more free parameters than in the simple scenario in [16], allows for a broader range of values of $|X|$ and θ_X as we stressed above, and there are other manifestations of new physics such as in modified values of some CKM parameters and in box contributions to four-fermion operators.

The answers to the questions posed at the beginning of our paper are as follows:

- The phase θ_X can be as large as found in [15, 16]. In fact as seen in Fig. 8 one finds typically
$$-160^\circ \leq \theta_X \leq 50^\circ \tag{5.1}$$
with a slightly increased range for the extended scan as seen in Fig. 10. Interestingly, there is a visible preference for negative values of θ_X that seem to be required by the $B \to \pi K$ data within a simpler new physics scenario discussed in [15, 16].

- However, among the allowed values of $|X|$, it is not easy to find simultaneously $|X| \approx 2.2$ and $\theta_X \approx -85^\circ$ as given in (1.9). Indeed for $\theta_X \approx -85^\circ$ the allowed value of $|X|$ in the constrained scan is typically lower than its SM value of 1.53 and only in the extended scan can it reach $|X| \approx 2.0$. Still, one cannot conclude from this finding that it is difficult to explain the $B \to \pi K$ data within the general MSSM, as the relation between the latter decays and $K \to \pi\nu\bar{\nu}$ in the general MSSM is rather weak. A very recent study of $B \to \pi K$ decays in the general MSSM can be found in [50].

- On the other hand for $-50^\circ \leq \theta_X \leq 50^\circ$, one can have $|X|$ as high as 7, implying that in this range of θ_X very large departures from the SM expectations are possible. A similar situation is found for $\theta_X = -(150 \pm 10)^\circ$ with $|X|$ reaching values as high as 7. This is illustrated in Figs. 8 and 10.

- It should be emphasized that values of $|X|$ significantly higher than 2, while excluded in the new physics scenario of [15, 16] through the data on $B \to X_s l^+ l^-$, are still allowed here because in the general MSSM there are no important correlations between B and K decays.

- The pattern of $Br(K_{\rm L} \to \pi^0\nu\bar{\nu}) \approx 3 \cdot 10^{-10}$ and $Br(K^+ \to \pi^+\nu\bar{\nu}) \approx 8 \cdot 10^{-11}$ found in [15, 16], although not easy to achieve within the general MSSM in the constrained scan, as seen in Figs. 7 and 9, can be obtained in the extended scan as shown in Fig. 10.

- More importantly, as seen in Figs. 7, 9 and 10, $Br(K^+ \to \pi^+\nu\bar{\nu})$ in the ball park of the central experimental value in (1.4) can be naturally obtained and simultaneously $Br(K_{\rm L} \to \pi^0\nu\bar{\nu})$ can be even larger than $Br(K^+ \to \pi^+\nu\bar{\nu})$. An example of supersymmetric parameters for which such pattern can be obtained is shown in table 3.

- Comparing Figs. 7 and 8 we observe that the experimental bound $Br(K^+ \to \pi^+\nu\bar{\nu})$ in (1.4) has a significant impact on the maximal allowed values of $|X|$ with essentially no impact on θ_X. This is not surprising as $K^+ \to \pi^+\nu\bar{\nu}$ is a CP-conserving decay. Clearly an improved upper bound on $Br(K_{\rm L} \to \pi^0\nu\bar{\nu})$ should have an important impact on the allowed values of θ_X.

- Finally, it is interesting to note that even in the general MSSM the angles β and γ of the unitarity triangle are rather constrained,

$$12^\circ \leq \beta \leq 27^\circ, \qquad 20^\circ \leq \gamma \leq 110^\circ \ . \tag{5.2}$$

  The constraint from the measured asymmetry $a_{\psi K_S}$ in (2.25) plays an important role here.

In summary, within the general MSSM large departures from the SM expectations for $K \to \pi\nu\bar{\nu}$ are still possible while satisfying all existing constraints. $Br(K^+ \to \pi^+\nu\bar{\nu})$ and $Br(K_{\rm L} \to \pi^0\nu\bar{\nu})$ can be both as large as few times 10^{-10} with $Br(K_{\rm L} \to \pi^0\nu\bar{\nu})$ often larger than $Br(K^+ \to \pi^+\nu\bar{\nu})$ and close to its model independent upper bound. In particular the results of a phenomenological study of enhanced electroweak penguins in [16] can be

obtained. The supersymmetric effects thus turn out to be larger than found in [12, 32], where typically $Br(K^+ \to \pi^+ \nu\bar{\nu}) \leq 1.7 \cdot 10^{-10}$ and $Br(K_{\rm L} \to \pi^0 \nu\bar{\nu}) \leq 1.2 \cdot 10^{-10}$ have been found. With regard to [12], this is partly due to the fact that these authors use the single MIA, while we use exact mass matrix diagonalization. The second reason is the exploration of a much larger space of parameters that was possible in a reasonable time only by using specially designed Monte Carlo techniques. On the other hand, [32] took into account RG effects between the GUT and weak scales, as is suitable for a high SUSY breaking scale, which allowed them to constrain the double mass insertion responsible for the large effects reported in [30]. Working in the completely general MSSM, we did not impose the RG constraint, while our exact mass diagonalization incorporates the second (and higher) orders in the MIA, in effect reinstating these large contributions to the extent allowed by the constraints listed in Subsect. 3.2.

In summary the large enhancements of $Br(K^+ \to \pi^+ \nu\bar{\nu})$ and $Br(K_{\rm L} \to \pi^0 \nu\bar{\nu})$ in the general MSSM found here are in the spirit of the findings of Colangelo and Isidori [30], except that we effectively incorporate not only the second but also higher order terms in the MIA, we explore much broader range of the space of supersymmetric parameters than done by these authors and we find the chargino box contributions more important than found in [30].

Acknowledgments
We would like to thank Oliver Brein for useful discussions on his adaptive scanning method, and for reading and comments on the corresponding parts of our manuscript. S.J. would like to thank the Fermilab theory group for their hospitality during the final stages of this work. T.E. has been supported by the German-Israeli Foundation under the contract G-698-22.7/2002. A.J.B. and J.R. have been supported in part by the German Bundesministerium für Bildung und Forschung under the contract 05HT4WOA/3 and the DFG Project Bu. 706/1-2. The work of S.J. is supported in part by the DFG Sonderforschungsbereich/Transregio 9 "Computergestützte Theoretische Teilchenphysik". J.R. was supported in part by Alexander von Humboldt Foundation and by KBN Grant 2 P03B 040 24 (2003-2005).

Appendix Contributions to the function X

In this appendix we collect the contributions to the functions X_L and X_R within the general MSSM in the mass eigenstates basis for particles and sparticles. To compactify our notation, we abbreviate fermion-scalar vertices as $i(V^L P_L + V^R P_R)$, with the actual values of V^L and V^R given by

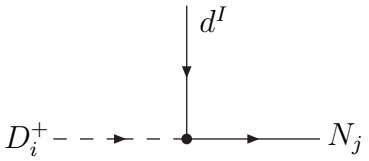

$$V^{LIij}_{dDN} = \frac{-e}{\sqrt{2} s_W c_W} Z_D^{Ii} \left[\frac{1}{3} Z_N^{1j} s_W - Z_N^{2j} c_W \right] + Y_d^I Z_D^{(I+3)i} Z_N^{3j}$$

$$V^{RIij}_{dDN} = \frac{-e\sqrt{2}}{3 c_W} Z_D^{(I+3)i} Z_N^{1j\star} + Y_d^I Z_D^{Ii} Z_N^{3j\star}$$

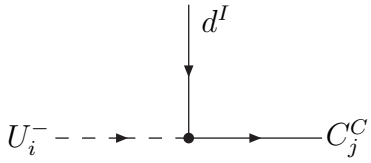

$$V_{dUC}^{LIij} = \left[\frac{-e}{s_W} Z_U^{Ji\star} Z_+^{1j} + Y_u^J Z_U^{(J+3)i\star} Z_+^{2j}\right] V_{JI}$$
$$V_{dUC}^{RIij} = -Y_d^I Z_U^{Ji\star} Z_-^{2j\star} V_{JI}$$

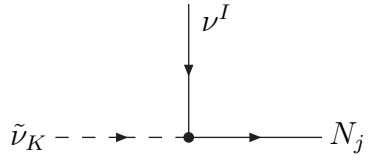

$$V_{\nu\tilde{\nu}N}^{LIKj} = \frac{e}{\sqrt{2} s_W c_W} Z_{\tilde{\nu}}^{IK\star} \left[Z_N^{1j} s_W - Z_N^{2j} c_W\right]$$
$$V_{\nu\tilde{\nu}N}^{RIKj} = 0$$

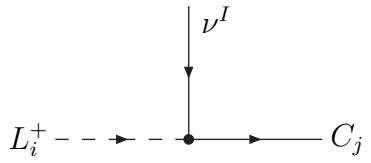

$$V_{\nu LC}^{LIij} = \frac{-e}{s_W} Z_L^{Ii} Z_-^{1j} - Y_e^I Z_L^{(I+3)i} Z_-^{2j}$$
$$V_{\nu LC}^{RIij} = 0$$

where $s_W = \sin\theta_W$, $c_W = \cos\theta_W$ and the definitions of the mixing matrices Z and the remaining vertices can be found in [49].

The contributions to X_L and X_R can be divided into two classes, generated by box-type and Z^0-penguin diagrams:

$$V_{3I} V_{3J}^\star [X_{L,R}]_{JIKL} = \sum_{i=SM,h,c,n,g} \left\{[B_{L,R}^i]_{JIKL} + [P_{L,R}^i]_{JI}\delta_{KL}\right\}. \tag{A.1}$$

This formula corresponds to a generalization of (2.3) to

$$\tilde{\mathcal{H}}_{\rm eff}^{(t)} = \sum_{K,L=1}^{3} V_{3I} V_{3J}^\star \left[[X_L]_{JIKL} (\bar{d}_J d_I)_{V-A} (\bar{\nu}_K \nu_L)_{V-A} + [X_R]_{JIKL} (\bar{d}_J d_I)_{V+A} (\bar{\nu}_K \nu_L)_{V-A}\right], \tag{A.2}$$

where for $K \to \pi\nu\bar{\nu}$ decays one should use $I = 1, J = 2$ and K, L are neutrino flavour indices (note that the subscript L on X_L refers to the chirality structure of the quark current and is no summation index). In general $X_{L,R}$ quantities defined in (A.1) carry lepton flavour indices. Only in the case when lepton flavour number is conserved in the slepton sector and the left- and right-slepton flavour diagonal mass parameters are identical for all three generations, the $X_{L,R}$ are to a good approximation (neglecting small terms proportional to lepton Yukawa couplings) universal, as assumed in (2.3). Relation between $X_{L,R}$ of (2.3) and of (A.2) is given by

$$[X_{L,R}]_{21KL} \equiv X_{L,R}\delta_{KL}. \tag{A.3}$$

In the numerical analysis in our paper we assume mentioned above simple flavour conserving structure of the slepton sector and use the definition (A.3).

Defining further

$$x_t = \frac{m_t^2}{M_W^2}, \qquad y_t = \frac{m_t^2}{M_H^2} \tag{A.4}$$

the non-vanishing box contributions read (summation over all indices other than J, I, K and L is understood)

$$[B_L^{SM}]_{JIKL} \;=\; -V_{3I} V_{3J}^\star 4 f_1(x_t)\, \delta_{KL} \tag{A.5}$$

$$[B_R^h]_{JIKL} = -V_{3I}V_{3J}^\star \frac{m_{d_I} m_{d_J} m_{e_K}^2 \tan^4\beta}{4M_W^2 M_H^2} f_1(y_t)\,\delta_{KL} \tag{A.6}$$

$$\begin{aligned}[B_L^c]_{JIKL} &= -\frac{M_W^2 s_W^4}{2e^4} V_{\nu LC}^{LLlm} V_{\nu LC}^{LKln\star} V_{dUC}^{LIkm} V_{dUC}^{LJkn\star} \\ &\times\ m_{C_m} m_{C_n} D_0(m_{C_m}^2, m_{C_n}^2, m_{U_k}^2, m_{L_l}^2)\end{aligned} \tag{A.7}$$

$$[B_R^c]_{JIKL} = \frac{M_W^2 s_W^4}{4e^4} V_{\nu LC}^{LLlm} V_{\nu LC}^{LKln\star} V_{dUC}^{RIkm} V_{dUC}^{RJkn\star} D_2(m_{C_m}^2, m_{C_n}^2, m_{U_k}^2, m_{L_l}^2) \tag{A.8}$$

$$\begin{aligned}[B_L^n]_{JIKL} &= -\frac{M_W^2 s_W^4}{4e^4} V_{dDN}^{LIkm} V_{dDN}^{LJkn\star} \Big[V_{\nu\tilde\nu N}^{LLNn} V_{\nu\tilde\nu N}^{LKNm\star} D_2(m_{N_m}^2, m_{N_n}^2, m_{D_k}^2, m_{\tilde\nu_N}^2) \\ &+\ 2V_{\nu\tilde\nu N}^{LLNm} V_{\nu\tilde\nu N}^{LKNn\star} m_{N_m} m_{N_n} D_0(m_{N_m}^2, m_{N_n}^2, m_{D_k}^2, m_{\tilde\nu_N}^2)\Big]\end{aligned} \tag{A.9}$$

$$\begin{aligned}[B_R^n]_{JIKL} &= \frac{M_W^2 s_W^4}{4e^4} V_{dDN}^{RIkm} V_{dDN}^{RJkn\star} \Big[V_{\nu\tilde\nu N}^{LLNm} V_{\nu\tilde\nu N}^{LKNn\star} D_2(m_{N_m}^2, m_{N_n}^2, m_{D_k}^2, m_{\tilde\nu_N}^2) \\ &+\ 2V_{\nu\tilde\nu N}^{LLNn} V_{\nu\tilde\nu N}^{LKNm\star} m_{N_m} m_{N_n} D_0(m_{N_m}^2, m_{N_n}^2, m_{D_k}^2, m_{\tilde\nu_N}^2)\Big]\end{aligned} \tag{A.10}$$

The non-vanishing penguin contributions read

$$[P_L^{SM}]_{JI} = V_{3I}V_{3J}^\star f_2(x_t) \tag{A.11}$$

$$[P_L^h]_{JI} = -V_{3I}V_{3J}^\star \frac{\cot^2\beta M_H^2}{2M_W^2} y_t f_1(y_t) \tag{A.12}$$

$$[P_R^h]_{JI} = V_{3I}V_{3J}^\star \frac{m_{d_I} m_{d_J} \tan^2\beta}{2M_W^2} f_1(y_t) \tag{A.13}$$

$$\begin{aligned}[P_L^c]_{JI} &= \frac{s_W^2}{8e^2} V_{dUC}^{LIkm} V_{dUC}^{LJin\star} \Big[2Z_-^{1m} Z_-^{1n\star} \delta_{ki} m_{C_m} m_{C_n} C_0(m_{U_k}^2, m_{C_m}^2, m_{C_n}^2) \\ &-\ Z_+^{1n} Z_+^{1m\star} \delta_{ki} C_2(m_{U_k}^2, m_{C_m}^2, m_{C_n}^2) + Z_U^{Nk} Z_U^{Ni\star} \delta_{mn} C_2(m_{C_m}^2, m_{U_k}^2, m_{U_i}^2)\Big]\end{aligned} \tag{A.14}$$

$$\begin{aligned}[P_R^c]_{JI} &= \frac{s_W^2}{8e^2} V_{dUC}^{RIkm} V_{dUC}^{RJin\star} \Big[2Z_+^{1n} Z_+^{1m\star} \delta_{ki} m_{C_m} m_{C_n} C_0(m_{U_k}^2, m_{C_m}^2, m_{C_n}^2) \\ &-\ Z_-^{1m} Z_-^{1n\star} \delta_{ki} C_2(m_{U_k}^2, m_{C_m}^2, m_{C_n}^2) - Z_U^{(N+3)k} Z_U^{(N+3)i\star} \delta_{mn} C_2(m_{C_m}^2, m_{U_k}^2, m_{U_i}^2)\Big]\end{aligned} \tag{A.15}$$

$$\begin{aligned}[P_L^n]_{JI} &= \frac{s_W^2}{8e^2} V_{dDN}^{LIkm} V_{dDN}^{LJin\star} \Big[Z_D^{(N+3)i} Z_D^{(N+3)k\star} \delta_{mn} C_2(m_{N_m}^2, m_{D_k}^2, m_{D_i}^2) \\ &+\ (Z_N^{4n} Z_N^{4m\star} - Z_N^{3n} Z_N^{3m\star}) \delta_{ki} C_2(m_{D_k}^2, m_{N_m}^2, m_{N_n}^2) \\ &+\ 2(Z_N^{4n\star} Z_N^{4m} - Z_N^{3n\star} Z_N^{3m}) \delta_{ki} m_{N_m} m_{N_n} C_0(m_{D_k}^2, m_{N_m}^2, m_{N_n}^2)\Big]\end{aligned} \tag{A.16}$$

$$\begin{aligned}[P_R^n]_{JI} &= -\frac{s_W^2}{8e^2} V_{dDN}^{RIkm} V_{dDN}^{RJin\star} \Big[Z_D^{Ni} Z_D^{Nk\star} \delta_{mn} C_2(m_{N_m}^2, m_{D_k}^2, m_{D_i}^2) \\ &+\ (Z_N^{4n\star} Z_N^{4m} - Z_N^{3n\star} Z_N^{3m}) \delta_{ki} C_2(m_{D_k}^2, m_{N_m}^2, m_{N_n}^2)\end{aligned}$$

$$+ \quad 2(Z_N^{4n} Z_N^{4m\star} - Z_N^{3n} Z_N^{3m\star})\delta_{ki} m_{N_m} m_{N_n} C_0(m_{D_k}^2, m_{N_m}^2, m_{N_n}^2)\Big] \tag{A.17}$$

$$[P_L^g]_{JI} = \frac{g_s^2 s_W^2}{3e^2} Z_D^{(M+3)i} Z_D^{(M+3)k\star} Z_D^{Ik} Z_D^{Ji\star} C_2(m_{\tilde{g}}^2, m_{D_k}^2, m_{D_i}^2) \tag{A.18}$$

$$[P_R^g]_{JI} = -\frac{g_s^2 s_W^2}{3e^2} Z_D^{Mi} Z_D^{Mk\star} Z_D^{(I+3)k} Z_D^{(J+3)i\star} C_2(m_{\tilde{g}}^2, m_{D_k}^2, m_{D_i}^2) \tag{A.19}$$

The loop functions appearing in these Wilson coefficients are given by

$$f_1(x) = \frac{x}{4(1-x)} + \frac{x \ln x}{4(1-x)^2} \tag{A.20}$$

$$f_2(x) = \frac{x(6-x)}{8(1-x)} + \frac{x(2+3x)\ln x}{8(1-x)^2} \tag{A.21}$$

$$C_0(x,y,z) = -\frac{y}{(x-y)(z-y)} \ln\frac{y}{x} + (y \leftrightarrow z) \tag{A.22}$$

$$\begin{aligned} C_2(x,y,z) &= \frac{2}{4-d} + \log 4\pi - \gamma_E + \ln\frac{\mu^2}{x} + 1 \\ &- \left\{ \frac{y^2}{(x-y)(z-y)} \ln\frac{y}{x} + (y \leftrightarrow z) \right\} \end{aligned} \tag{A.23}$$

$$D_0(x,y,z,t) = \frac{-y}{(y-x)(y-z)(y-t)} \ln\frac{y}{x} + (y \leftrightarrow z) + (y \leftrightarrow t) \tag{A.24}$$

$$D_2(x,y,z,t) = \frac{-y^2}{(y-x)(y-z)(y-t)} \ln\frac{y}{x} + (y \leftrightarrow z) + (y \leftrightarrow t) \tag{A.25}$$

Infinite and μ-dependent terms in C_2 always cancels out in flavour off-diagonal penguins after summation over squark, chargino and neutralino mixing matrices. We recall that $f_1(x) = B_0(x)$ and $f_2(x) = C_0(x)$ in the notation of [7].

References

[1] G. Buchalla and A. J. Buras, Nucl. Phys. **B398** (1993) 285.

[2] G. Buchalla and A. J. Buras, Nucl. Phys. **B400** (1993) 225.

[3] M. Misiak and J. Urban, Phys. Lett. **B451** (1999) 161.

[4] G. Buchalla and A. J. Buras, Nucl. Phys. **B548** (1999) 309.

[5] G. Buchalla and A. J. Buras, Nucl. Phys. **B412** (1994) 106.

[6] A. J. Buras, F. Schwab and S. Uhlig, arXiv:hep-ph/0405132.

[7] G. Buchalla, A. J. Buras and M. E. Lautenbacher, Rev. Mod. Phys. **68** (1996) 1125; A. J. Buras, hep-ph/9806471.

[8] G. Isidori, eConf **C0304052**, WG304 (2003), arXiv:hep-ph/0307014.

[9] R. Fleischer, Phys. Rep. **370** (2002) 537 [arXiv:hep-ph/0207108].

[10] M. Ciuchini and L. Silvestrini, Phys. Rev. Lett. **89** (2002) 231802.

[11] M. Neubert, arXiv:hep-ph/0405105.

[12] A.J. Buras, A. Romanino and L. Silvestrini, Nucl. Phys. **B520**, (1998) 3.

[13] G. D'Ambrosio and G. Isidori, Phys. Lett. B **530** (2002) 108 [arXiv:hep-ph/0112135].

[14] S. H. Kettell, L. G. Landsberg and H. H. Nguyen, arXiv:hep-ph/0212321.

[15] A. J. Buras, R. Fleischer, S. Recksiegel and F. Schwab, Phys. Rev. Lett. **92** (2004) 101804.

[16] A. J. Buras, R. Fleischer, S. Recksiegel and F. Schwab, arXiv:hep-ph/0402112.

[17] S. Adler *et al.*, Phys. Rev. Lett. **79** (1997) 2204, Phys. Rev. Lett. **84** (2000) 3768.

[18] S. Adler *et al.*, Phys. Rev. Lett. **88**, (2002) 041803. S. Adler *et al.* [E787 Collaboration], arXiv:hep-ex/0403034.

[19] V. V. Anisimovsky *et al.* [E949 Collaboration], Phys. Rev. Lett. **93**, (2004) 031801; arXiv:hep-ex/0403036.

[20] http://www.fnal.gov./projects/ckm/documentation/public/proposal/proposal.html.

[21] http://na48.web.cern.ch/NA48/NA48-3/index.html

[22] http://www-ps.kek.jp/jhf-np/LOIlist/LOIlist.html.

[23] A. Alavi-Harati *et al.* [The E799-II/KTeV Collaboration], Phys. Rev. **D61**,(2000) 072006.

[24] http://www-ps.kek.jp/e391.

[25] L. Littenberg, arXiv:hep-ex/0212005. D. Bryman, arXiv:hep-ex/0206072.

[26] Y. Grossman and Y. Nir, Phys. Lett. **B398**, (1997) 163.

[27] G. Buchalla and A. J. Buras, Phys. Lett. **B333**, (1994) 221.

[28] S. Rai Choudhury, N. Gaur and A. S. Cornell, arXiv:hep-ph/0402273.

[29] G. Isidori, C. Smith and R. Unterdorfer, arXiv:hep-ph/0404127.

[30] G. Colangelo and G. Isidori, JHEP **9809** (1998) 009.

[31] A.J. Buras and L. Silvestrini, Nucl. Phys. **B546** (1999) 299.

[32] A.J. Buras, G. Colangelo, G. Isidori, A. Romanino and L. Silvestrini, Nucl. Phys. **B566** (2000) 3 [arXiv:hep-ph/9908371].

[33] G. Buchalla, G. Hiller and G. Isidori, Phys. Rev. **D63** (2001) 014015;
D. Atwood and G. Hiller, LMU-09-03 [arXiv:hep-ph/0307251].

[34] L.J. Hall, V.A. Kostelecky and S. Raby, Nucl. Phys. **B267** (1986) 415.

[35] F. Gabbiani, E. Gabrielli, A. Masiero and L. Silvestrini, Nucl. Phys. **B477** (1996) 321.

[36] M. Misiak, S. Pokorski and J. Rosiek, Adv. Ser. Direct. High Energy Phys. **15** (1998) 795 [arXiv:hep-ph/9703442].

[37] Y. Grossman, Y. Nir and R. Rattazzi, Adv. Ser. Direct. High Energy Phys. **15** (1998) 755.

[38] Y. Nir and M. P. Worah, Phys. Lett. **B423** (1998) 319 [arXiv:hep-ph/9711215].

[39] O. Brein, PITHA-04-12 [arXiv:hep-ph/0407340].

[40] G. P. Lepage, J. Comput. Phys. **27** (1978) 192; G. P. Lepage, CLNS-80/447

[41] L. Wolfenstein, *Phys. Rev. Lett.* **51** (1983) 1945.

[42] S. Eidelman *et al.*, Phys. Lett. **B 592** (2004) 1.

[43] J. A. Casas and S. Dimopoulos, Phys. Lett. B **387** (1996) 107 [arXiv:hep-ph/9606237].

[44] J. A. Casas, A. Lleyda and C. Munoz, Nucl. Phys. B **471** (1996) 3 [arXiv:hep-ph/9507294]; J. A. Casas, arXiv:hep-ph/9707475.

[45] D.E. Knuth, "The Art of Computer Programming, Vol. 2: Seminumerical Algorithms", 3rd edition, Addison-Wesley 1998.

[46] "Monte Carlo Simulation of Radiative Processes in Electron - Positron Scattering" by Ronaldus H.P. Kleiss (Leiden U.),. RX-988 (LEIDEN), INIS-mf-7671, Jun 1982. 86pp. Ph.D. Thesis.

[47] "Toward a Universal C Random Number Generator" by George Marsaglia and Arif Zaman. C Florida State University Report: FSU-SCRI-87-50 (1987).

[48] F. James, Comput. Phys. Commun. **60** (1990) 329.

[49] J. Rosiek, *Phys. Rev.* **D41** (1990) 3464, *erratum* hep-ph/9511250.

[50] S. Khalil and E. Kou, arXiv:hep-ph/0407284.